

博士論文

**Setd1a plays pivotal roles for the survival and proliferation of
retinal progenitors via histone modifications of Uhrf1**

(Setd1a は Uhrf1 のヒストン修飾を制御することで網膜前駆
細胞の生存や増殖において重要な役割を果たしている)

鄧 小月

DENG XIAOYUE

博士論文

Setd1a plays pivotal roles for the survival and proliferation of retinal progenitors via histone modifications of Uhrf1

(Setd1a は Uhrf1 のヒストン修飾を制御することで網膜前駆細胞の生存や増殖において重要な役割を果たしている)

所属：医学系研究科 分子細胞生物学専攻

指導教員：渡邊 すみ子

申請者：DENG XIAOYUE (トウ ショウゲツ)

Table of Contents

Abstract	3
Introduction	4 - 13
Materials and Methods	14 - 18
Results	19 - 41
Discussion	42 - 47
Conclusion	48
References	49 - 56
Acknowledgements	57

Abstract

The trimethylation of histone H3 at lysine 4 (H3K4me3) facilitates transcriptional gene activation, and *Setd1a* is the methyltransferase specific to H3K4. H3K4me3 has been reported to regulate rod photoreceptor differentiation; however, the roles H3K4me3 plays in retinal progenitor cell proliferation and differentiation during early retinal development remain unclear. Using an *in vitro* retinal explant culture system, we suppressed the expression of *Setd1a* by introducing shSetd1a. We found that *Setd1a* depletion resulted in increased apoptosis and proliferation failure in late retinal progenitor cells. Expression of wild-type SETD1A, but not SETD1A that lacked the catalytic SET domain, reversed the shSetd1a-induced phenotype, indicating that *Setd1a* contributes to the survival and proliferation of retinal cells by regulating histone methylation. RNA Sequencing of shSetd1a-expressing and control retinal cells revealed that proliferation-related genes were downregulated upon shSetd1a expression. Based on publicly available H3K4me3-ChIP Sequencing data of retinal development, we identified *Uhrfl* as a candidate target gene of *Setd1a*. The expression of shSetd1a led to a decrease in *Uhrfl* transcript levels and reduced H3K4me3 levels at the *Uhrfl* locus in the retina. Increased apoptosis and the suppression of proliferation in late retinal progenitor cells were observed in retinal explants expressing shUhrfl, similar to the outcomes observed in shSetd1a-expressing retinas. The overexpression of UHRF1 did not rescue shSetd1a-induced apoptosis, but was able to reverse the suppression of proliferation. These results indicate that *Setd1a* regulates *Uhrfl* expression, and these two molecules cooperate to regulate retinal progenitor cell survival and proliferation.

Introduction

1. Development of vertebrate retina

The vertebrate retina is a part of the central nervous system, and retinal explant culture served an excellent model to analyze molecular mechanisms of development. During retinal development, retinal progenitor cells (RPCs) are multipotent cells that proliferate and differentiate into six types of neurons, namely amacrine cells, bipolar cells, horizontal cells, retinal ganglion cells, photoreceptor cells, and one type of glial cell called Müller-glia [1]. Those cell types are distributed in three nuclear layers separated by two plexiform layers. RGCs occupy the innermost nuclear layer, namely ganglion cell layer (GCL), and photoreceptors constitute the outer nuclear layer (ONL). The remaining four cell types form the inner nuclear layer (INL), which is located between the GCL and the ONL [2]. The temporal order of the production of each retinal cell is known to be highly regulated and conserved among species [3], [4] (Fig. 1). In mice, retinogenesis starts at embryonic day 11 (E11). Specifically, the RPCs are separated into early and late RPCs with a clear segregation occurring between E16 and E18 [5]. At the optic vesicle stage of eye development, early RPCs appear and tend to symmetrically divide to increase the pool of RPCs. Then, the cells begin to asymmetrically divide and give rise to the early-born retinal cell types. Late RPCs continue to asymmetrically divide and tend to undergo terminal cell cycle exit, differentiating into the late-born retinal cell types, which include the bipolar cells, certain subtypes of amacrine cells, as well as photoreceptor cells and Müller-glia [6], [7].

The molecular mechanisms by which cell fate is determined and maturation is accomplished have been intensively investigated, and much attention has been paid to the roles of transcription factors in the retinal development [4], [8]. The particular order of genesis of retinal cells is evolutionarily conserved, suggesting that temporally regulated mechanisms are a major factor that drives cell fate outcomes [9], [10]. RPCs are extremely heterogeneous and many differences in gene expression within RPCs were found. Previous studies have suggested that RPCs that express neurogenic basic helix-loop-helix factors such as *Ng2*, *Atoh7*, and *Olig2* may be biased to generate specific neuronal subtypes [10]–[12]. For example, a study using clonal lineage analysis to investigate the progeny of a subset of RPCs, and found that both embryonic and postnatal *Olig2*⁺ RPCs made terminal divisions, which were biased toward specific cell fates [12]. A recent study, using single-cell RNA sequencing, profiled ten developmental stages encompassing the full course of retinal neurogenesis. As a result, they identified previously established markers of both early (*Fgf15* and *Sfrp2*) and late (*Crym* and *Car2*) RPCs [13] and a host of previously unidentified markers of early versus late RPCs, including the late RPC-enriched nuclear factor I (NFI) transcription factors (*Nfia*, *Nfib*, and *Nfix*) for the reasons that they control cell-cycle exit and generation of late-born retinal cell types [5].

2. Epigenetic modifications

Epigenetic modifications are defined as stable and heritable alterations in gene expression and cellular function without changes to the original DNA sequence [14]. They are highly

involved in biological processes via regulating gene expression, including DNA methylation, histone post-translational modifications and microRNAs [15]. As one of the most widely studied epigenetic modifications, DNA methylation can occur in different regions of the genome. CpG islands, the regions that contain a cluster of CpG dinucleotide repeats, are normally unmethylated at promoters to allow transcription initiation [16]. On the other hand, repetitive sequences appear to be hypermethylated, preventing chromosomal instability, translocations and gene disruption [17]. DNA methylation is mediated by catalytic enzymes of the DNMT family, which is categorized into *de novo* DNMTs (*Dnmt3a* and *Dnmt3b*) and maintenance DNMTs (*Dnmt1*) [18]. *Dnmt1* is preferentially methylate hemimethylated sites that are generated during DNA replication. The ubiquitin-like plant homeodomain and RING finger domain-containing protein 1 (*Uhrf1*) could perform a similar function, recruiting *Dnmt1* to hemimethylated DNA and maintain the global DNA methylation during DNA replication [19]–[21].

Histone post-translational modifications (e.g. methylation, acetylation, ubiquitylation, and sumoylation) orchestrate gene expression by modifying the N-terminal tails of histones and altering chromatin structure [22]. Different types of histone modifications have diverse functions on gene expression regulation, DNA repair, DNA replication, alternative splicing and chromosome condensation, which is related to distinct location and varying degree [23]–[25]. In terms of transcriptional state, actively transcribed euchromatin is enriched with active histone marks, whereas inactive heterochromatin is characterized by inactive histone marks [26], [27]. For example, histone H3 methylation at lysine 4 (H3K4) is associated with gene

activation, and three statuses of lysine methylation, namely mono-, di-, tri- methyl groups (me1/2/3), contribute to additional layer of complexity in chromatin remodeling events [28], whereas trimethylated histone H3 lysine 27 (H3K27me3) around promoter region mediates gene repression [29]. Epigenetic chemical modifications are addressed by several kinds of protein families that are categorized as writers, erases and readers. Writers reside the chemical modifications to specific loci; erasers function as removal of them; readers recognize specific domains and bind to them [30] (Fig. 2). For example, to regulate H3K4 methylation, writers refer to histone lysine methyltransferases (KMT2A, KMT2C, KMT2D, KMT2F), while erasers are histone lysine demethylases (KDM1A, KDM5A, KDM5B, KDM5C) [31].

It is well documented that epigenetic modification players have strong connection with each other. In the case of DNMT3L, one of the DNA methyltransferases belongs to DNMT family, specifically interacts with histone H3, and this interaction is strongly inhibited by H3K4 methylation [32]. Another example is that G9a/GLP suppresses transcription by independently inducing both H3K9 and DNA methylation [33]. Furthermore, unmethylated CpG islands generate a transcriptional friendly chromatin structure by recruiting *Cfp1*, which associates with histone H3K4me3 methyltransferase *Setd1a* or methyltransferases *Setd1a* and *Setd1b* [34]. *Uhrf1*, contributing to DNA methylation maintenance, was proved to regulate active transcriptional marks via H3K4me3 with *Setd1a* [35].

3. Methyltransferases and demethylases in retinal development and disease

The contributions of epigenetic modifications, such as DNA methylation and histone modifications, to retinal development are becoming clearer [36]–[38]. We have been studying epigenetic histone modifications during retinal development and, with others, found that both H3K4 and H3K27 were highly specific to retinal cell type. Additionally, analyses of knockout mice have revealed the functions of enzymes involved in these processes, especially H3K27 methylation. Retina-specific knockout of *Ezh2* or *Utx*, which are H3K27 methylation enzymes, affected the proliferation or/and maturation of certain retinal subsets [39], [40]. Among the nine histone lysine methyltransferases and five histone lysine demethylases that involved in H3K4 methylation [41], *Kdm5b*, a demethylation enzyme, participates in the determination of rod photoreceptor cell fate [42]. Though we found high levels of H3K4me3 in photoreceptor-related genes in rod photoreceptor lineage [43], the involvement of H3K4 methylation in early retinal development is not well-documented.

Setd1a (*Kmt2f*) encodes the member of a SET/COMPASS complex [44] and catalyzes H3K4 methylation [45]. *Setd1a* contains a Su(var)-3-9, Enhancer-of-zeste, Trithorax (SET) domain at its C-terminus, which is a catalytic domain responsible for H3K4 histone methyltransferase activity [31], [46], [47] (Fig. 3). The *Set1* complex or COMPASS is conserved across different species through evolution. Human SETD1A and SETD1B are two paralogs but interact with unique proteins [48] (Fig. 4). *Setd1a* is required for embryonic, epiblastic, and neural stem cell survival, and gene knockout of *Setd1a* in mice led to rapid losses of bulk H3K4 methylation and a severe decrease in cell proliferation during embryonic development [49]. *Setd1a* also helps to maintain genome stability under replication stress

through its methylation function [50], [51]. In addition, *Setd1a* has non-enzymatic role, such as regulating DNA damage-response genes via its FLOS domain [52]. *Setd1a* is highly expressed in the murine brain, especially in the neocortex [53]. *Setd1a* haploinsufficiency affects the development of cortical axons, dendrites, and spines, resulting in cognitive defects [54], [55]. Mutations of *Setd1a* have been found in human neurodevelopmental disorders such as schizophrenia [56], [57].

In the retina, the roles *Setd1a* plays in retinal development or diseases have not been documented. In this study, we examined the functions of *Setd1a* via shRNA-mediated downregulation of *Setd1a* during retinal development. We found that *Setd1a* is essential for the survival and proliferation of late-stage RPCs. RNA Sequencing (RNA-Seq) was performed to compare gene expression patterns between control and shSetd1a-expressing retinal cells, and *Uhrfl* was identified as a possible target. *Uhrfl* loss-of-function also resulted in apoptosis and proliferation failure. Interestingly, ectopic expression of UHRF1 reversed shSetd1a-induced suppression of proliferation but not the induction of apoptosis. Our results indicate that *Setd1a* and *Uhrfl* play critical roles during early retinal development.

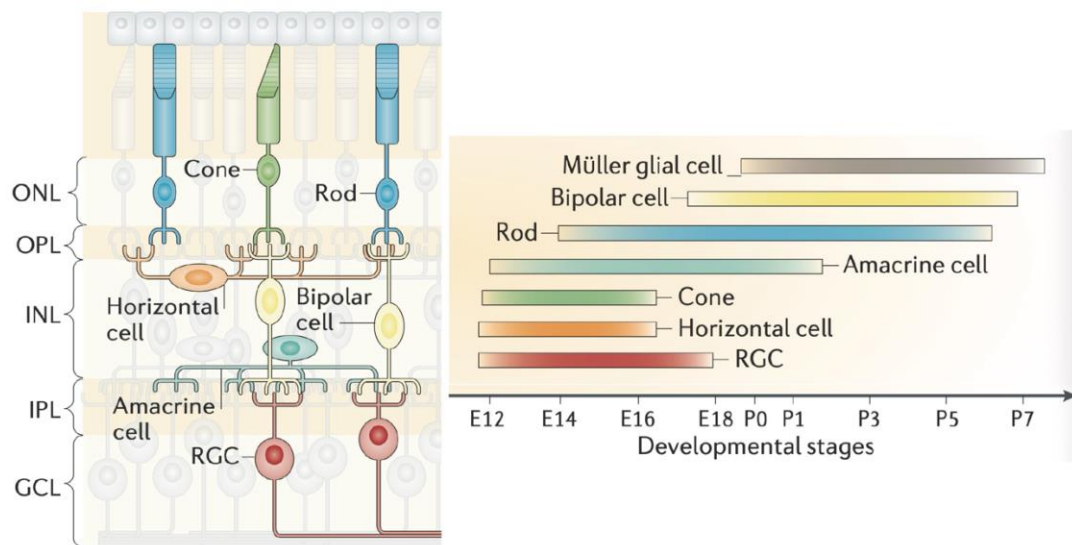


Figure 1. Retinal cell types and their birth order.

Left: A cross-section of the retina. The retina is organized into three layers of cell bodies (the outer nuclear layer (ONL), the inner nuclear layer (INL) and the ganglion cell layer (GCL)) and two layers of neuropil (the outer plexiform layer (OPL) and the inner plexiform layer (IPL)). Retinal neurons comprise primary sensory cells (rods and cones), interneurons (horizontal cells, bipolar cells and amacrine cells) and output neurons (retinal ganglion cells (RGCs)). There are many subtypes of each type of neuron that vary not only in terms of their functions and features but also in their frequencies. Each cell type is distributed such that the entire retina has the full complement of cell types, and each subtype is evenly spaced or tiled across the retina. Right: The birth dates of each of the major cell types in the rat and mouse retina are indicated. Classical ^3H -thymidine birth dating has shown the same overall order of retinal cell birth dates across many species (Adapted from reference 4).

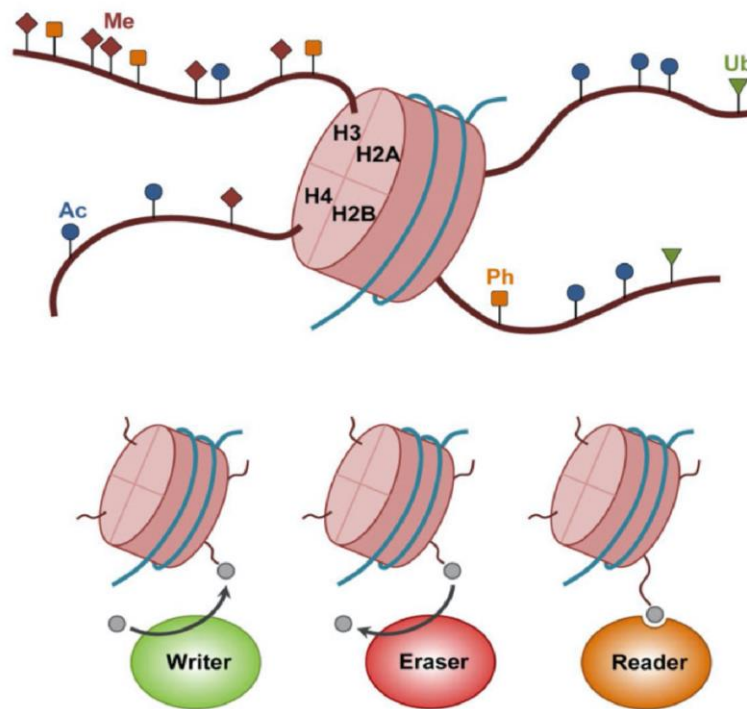


Figure 2. Writers, erasers and readers.

The basic functional unit of chromatin is the nucleosome, which is composed of DNA wrapped around histones (H2A, H2B, H3 and H4). Core histone tails are projected from nucleosomes and are subject to post-translational modifications (PTMs). These include methylation (Me), acetylation (Ac), phosphorylation (Ph) and ubiquitination (Ub). The main epigenetic regulators can be categorized as writers, erasers and readers of PTMs. Epigenetic writers are responsible for the addition of chemical modifications. Epigenetic erasers catalyze the removal of the covalent modifications. Epigenetic readers are proteins with specific domains that recognize and bind to particular modifications (Adapted from reference 31).

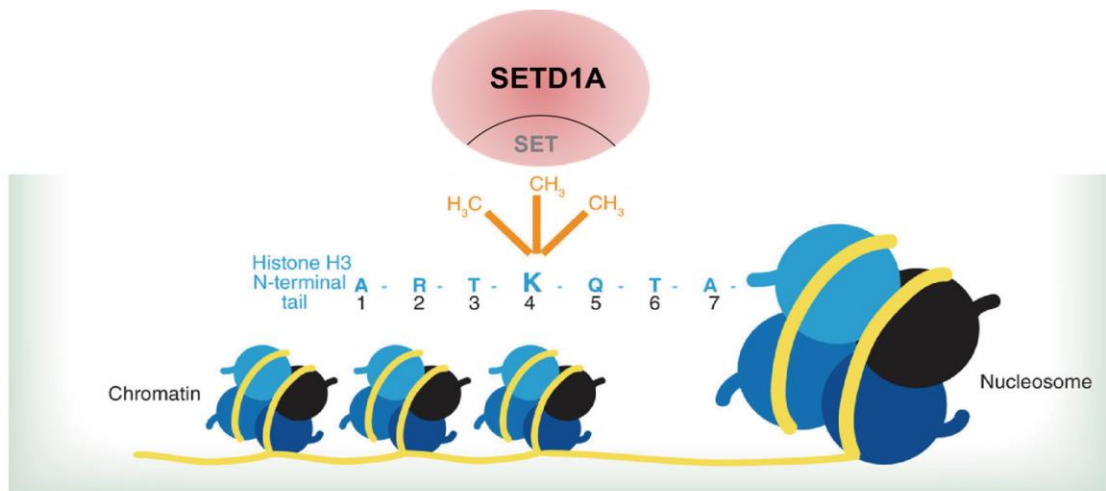


Figure 3. H3K4me3 methyltransferase SETD1A.

The first seven amino acids of the N-terminal tail of histone H3 (light blue) are extending from a representative nucleosome. Lysine (K) 4 can be differentially methylated (orange) by the writers; methyltransferase SETD1A (light red) ‘write’ methyl marks through catalytic SET domain (gray) (Adapted from reference 32).

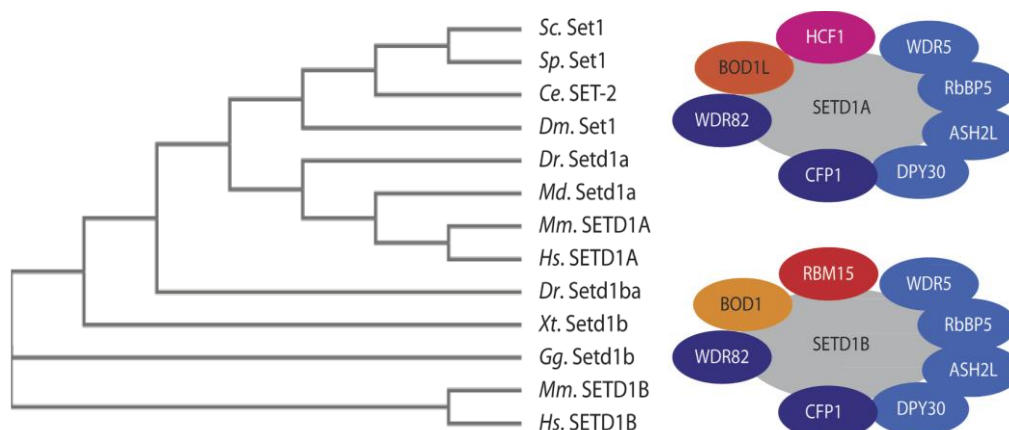


Figure 4. Set1 proteins are conserved in evolution.

Left: Phylogenetic analysis of Set1 from different species using Clustal Omega. The alignment was based on the sequences of the n-SET, SET and post-SET domain of *Saccharomyces cerevisiae* (Sc), *Schizosaccharomyces pombe* (Sp), *Caenorhabditis elegans* (Ce), *Drosophila melanogaster* (Dm), *Danio rerio* (Dr), *Xenopus tropicalis* (Xt), *Gallus gallus* (Gg), *Monodelphis domestica* (Md), *Mus musculus* (Mm), *Homo sapiens* (Hs). Right: In mammals SETD1A and SETD1B have unique members in addition to common subunits (WDR5, RbBP5, ASH2L, DPY30, CFP1, WDR82). SETD1A associates with BOD1L and HCF1, whereas SETD1B with BOD1 and RBM15 (Adapted from reference 49).

Materials and Methods

Animal

All animal experiments were approved by the Animal Care Committee of the Institute of Medical Science, University of Tokyo, and conducted in accordance with the ARVO (Association for Research in Vision and Ophthalmology) statement for the use of animals in ophthalmic and vision research. Institute of Cancer Research (ICR) mice were obtained from Japan SLC Co.

RT-qPCR and shRNA plasmids construction

Total RNA was purified from the mouse retina using Sepasol RNA I Super G (Nacalai tesque), and cDNA was synthesized using ReverTra Ace qPCR RT Master Mix (TOYOBO).

Quantitative PCR (qPCR) was performed by the SYBR Green-based method with the Roche Light Cycler 96 (Roche Diagnostics). *Actb* and *Glyceraldehyde 3-phosphate dehydrogenase*

(*Gapdh*) were used as internal controls. Primer sequences are as follows: *Actb*_f: 5'-

ccaaccgcgagaagatga-3', *Actb*_r: 5'-ccagaggcgctacaggtag-3', *Gapdh*_f: 5'-

tgaccacagtccatgccatc-3', *Gapdh*_r: 5'-cataccaggaaatgagcttgac-3', *Setd1a*_f: 5'-

ggcaacatcattcatgccca-3', *Setd1a*_r: 5'-gataggcagctgtgtccgag-3', *Setd1b*_f: 5'-

ggatgaaggcatcggttagca-3', *Setd1b*_r: 5'-gatcaccttggcgtagcagt-3'. Construction of the shRNA

plasmids were done as described previously [58]. The target sequences (shSetd1a_1st: 5'-

aaggatatgtgccgaaatatgg-3', shSetd1a_2nd: 5'-aagctaaaccagctcaagtttcg-3', shUhrf1_1st: 5'-

aaggagctttccagtgcattctgc-3', and shUhrf1_2nd: 5'-aagcggatgacaagactgtgtgg-3', shSetd1b: 5'-

aagttacaagttgatgattgacc-3') were determined by using siDirect ([http:// sidirect2.rnai.jp](http://sidirect2.rnai.jp)).

Knockdown efficiency of each shRNA was examined in the retinal explant culture. The 1st

and 2nd shRNAs for both *Setd1a* and *Uhrfl* showed essentially the same results in the critical experiment, and representative data obtained by shRNA_firsts are shown in the figures.

DNA construction of overexpression of *Setd1a* and *Uhrfl*

Full-length *Setd1a* cDNA was cloned by PrimeSTAR GXL DNA Polymerase (TAKARA, Japan) using cDNA from mouse retina. PCR product was subcloned into pGEM-T Easy vector (Promega, USA). shSetd1a-resistant *Setd1a* contains substitutions of the third bases of four amino acid, which do not affect the encoded amino acids by inverse PCR using the KOD-Plus-Mutagenesis Kit (Toyobo, Japan). The resultant fragment was substituted with the corresponding region of wild-type *Setd1a* by *XhoI* and *EcoRV* sites. *Setd1a* mutant lacking SET domain (from AA 1577 to 1700) was constructed by KOD-Plus-Mutagenesis Kit (Toyobo, Japan). The full-length *Uhrfl_HA* was purchased from Sino Biological (MG53591-CY, China), and shUhrfl-resistant *Uhrfl* was made by inverse PCR using the KOD-Plus-Mutagenesis Kit (Toyobo, Japan). All the cDNAs for over-expression were subcloned into pCAG-KS.

Electroporation and retinal explant culture

In vitro electroporation and retinal explant culture were performed as described previously [59], [60]. To trace plasmid-transfected cells, we co-transfected an enhanced green fluorescent protein (EGFP)-expression plasmid (pCAG-EGFP) with shRNA expression plasmid. Total amount of plasmids used for electroporation was 100 µg for each retina and composition of plasmids is empty or shRNA (70 µg) and pCAG-EGFP (30 µg) or shRNA (40 µg), pCAG or pCAG-rescue cDNA (40 µg) and pCAG-EGFP (20 µg). In some cases, to

avoid apoptosis, retinas were cultured for 3 days in the presence of pan-Caspase inhibitor Z-VAD-FMK (AdooQ BioScience, A12373) at 20 μ M in the final concentration. For all the samples, we performed at least three independent electroporation with the same condition and counted cells from two or three sections in each sample.

Immunohistochemistry

Immunostaining of frozen sections was done as described previously [59], [60]. Primary antibodies used were mouse monoclonal antibodies against Ki67 (BD Bioscience, 550609), HuC/D (Molecular Probes, A-21271), TFAP2A (DSHB, 3B5), cyclin D3 (Santa Cruz, sc-182), NR2E3 (photoreceptor-specific nuclear receptor, PNR) (PP-H7223-00, PPMX), Glutamine synthetase (GS) (MAB302; Chemicon), SETD1A (Abcam, ab70378) and 5-methylcytosine (5mC) (Active Motif, 39649), sheep polyclonal antibody against Chx10 (Exalha Biologicals), goat polyclonal antibody against BRN3B (Santa Cruz, sc-6026), chick polyclonal antibody against GFP (Clontech), and rabbit polyclonal antibody against active Caspase 3 (Promega, G748A). To optimize 5mC signal, careful titration of hydrochloric (HCl) acid treatment before blocking and labelling was performed. Briefly, after wash with PBS for 10 minutes, retinal sections were permeabilized with 0.1% Triton X-100 for 10 minutes at room temperature and denatured for 15 minutes with freshly made 2 N HCl at 37°C. Then, retinal sections were neutralized with 0.1 M Tris-HCl (pH 8.0) for 10 minutes at room temperature. Nuclei were counterstained with 4',6-diamidino-2-phenylindole, dihydrochloride (DAPI). Sections were then treated with Alexa-488- or Alexa-594-conjugated appropriate secondary antibodies. Photos were taken under observation using Zeiss Axio Image M1 and Axio Image M2.

RNA Sequencing (RNA-Seq)

Retinas (E17) were electroporated with either control or shSetd1a plasmid and cultured for 2 days. EGFP positive cells ($\sim 3 \times 10^4$ cells for 1 sample) were collected by a cell sorter, FACS Aria II (BD Biosciences) as described [61]. 4 samples were prepared for both control and shSetd1a. Total RNA was extracted using Sepasol RNA I Super G (Nacalai tesque) and qualified by using a 2100 Bioanalyzer (Agilent Technologies). Using 1 ng of total RNA, cDNA was prepared and amplified by PCR by SMART-Seq v4 Ultra Low Input RNA Kit for Sequencing (TAKARA) according to the manufacturer's instructions. The RNA-Seq libraries were prepared using the amplified cDNA and Nextera XT DNA Sample Preparation Kit (Illumina). 36 bp of single read sequencing was conducted by HiSeq3000 sequencer (Illumina).

Data analysis of RNA-Seq results

Sequenced reads were mapped to the mouse transcriptome (GENCODE GRCm38.p6) with salmon v0.11.3 [62]. Salmon output was converted using wasabi v0.3 [62] and loaded into sleuth v0.30.0 [63] for further downstream analysis including statistical testing and visualization. Gene ontology (GO) term enrichment analysis was performed using the Database for Annotations, Visualization and Integrated Discovery (DAVID) with "GO_BP" (gene ontology biological processes) terms [64], [65].

Chromatin immunoprecipitation (ChIP)-qPCR assay

ChIP-qPCR was done as previously described [66]. Antibodies used for ChIP assay were as follows: anti-histone H3 tri-methyl Lys4 (H3K4me3) antibody (Active motif), and rabbit

control IgG (Cell Signaling). Primer sequences are as follows; *Uhrfl*_Primer A_F 5'-aggtcaaagttgtccagctca-3', R 5'-gggagacttcacccaatt-3', *Uhrfl*_Primer B_F 5'-gctcacttgggtcttcagcc-3', R 5'-ctctgcagatctcaccac-3', *Uhrfl*_Primer C_F 5'-gagattcaattgtcgcgcc-3', R 5'-aaactcacctgaacccacc-3'.

Re-analysis of public ChIP-seq data

H3K4me3 ChIP-seq reads from P0 retina and the corresponding input reads from GSE87064 [67] were aligned to GRCm38 by Bowtie2 2.4.1 [68] with default parameters. The aligned data were converted to BAM files by SAMtools 1.10 [69], [70]. MACS2 2.2.71 [71] was then used for peak calling with the cutoff of $q < 0.05$, and the peaks were annotated by ChIPseeker 1.5.1 [72].

Statistical analysis

Statistical analysis was performed using R software (The R Foundation for Statistical Computing, Vienna, Austria). The p-values were calculated by Student's T-test or Tukey's test as indicated in the figure legend.

Results

1. Changes in *Setd1a* expression levels during retinal development

The expression pattern of *Setd1a* transcripts during retinal development was examined via RT-qPCR using RNAs extracted from whole mouse retinas at different developmental stages (Fig. 5A, left panel). Previous RNA-Seq analysis of developing mouse retinas (GSE87064) confirmed that *Setd1a* expression levels gradually decreased during retinal development (Fig. 5A, right panel). *Setd1a* transcript levels remained stable from embryonic day 14 (E14) to postnatal day 1 (P1), then gradually decreased to approximately half the levels observed during the embryonic period at P3. Levels subsequently stayed low until week 8.

The spatial expression pattern of the SETD1A protein was then examined via immunohistochemistry using frozen retinal sections. SETD1A was expressed at high levels across the entire embryonic retina, and gradually disappeared from the neuroblast layer during the postnatal stages (Fig. 5B). Staining with Ki67 proliferation antigen revealed that SETD1A was expressed in both proliferating and post-mitotic cells. Furthermore, SETD1A was expressed in amacrine cells (HuC/D; Fig. 5C) and retinal ganglion cells (Brn3b; Fig. 5D) but not in bipolar cells (Chx10; Fig. 5E).

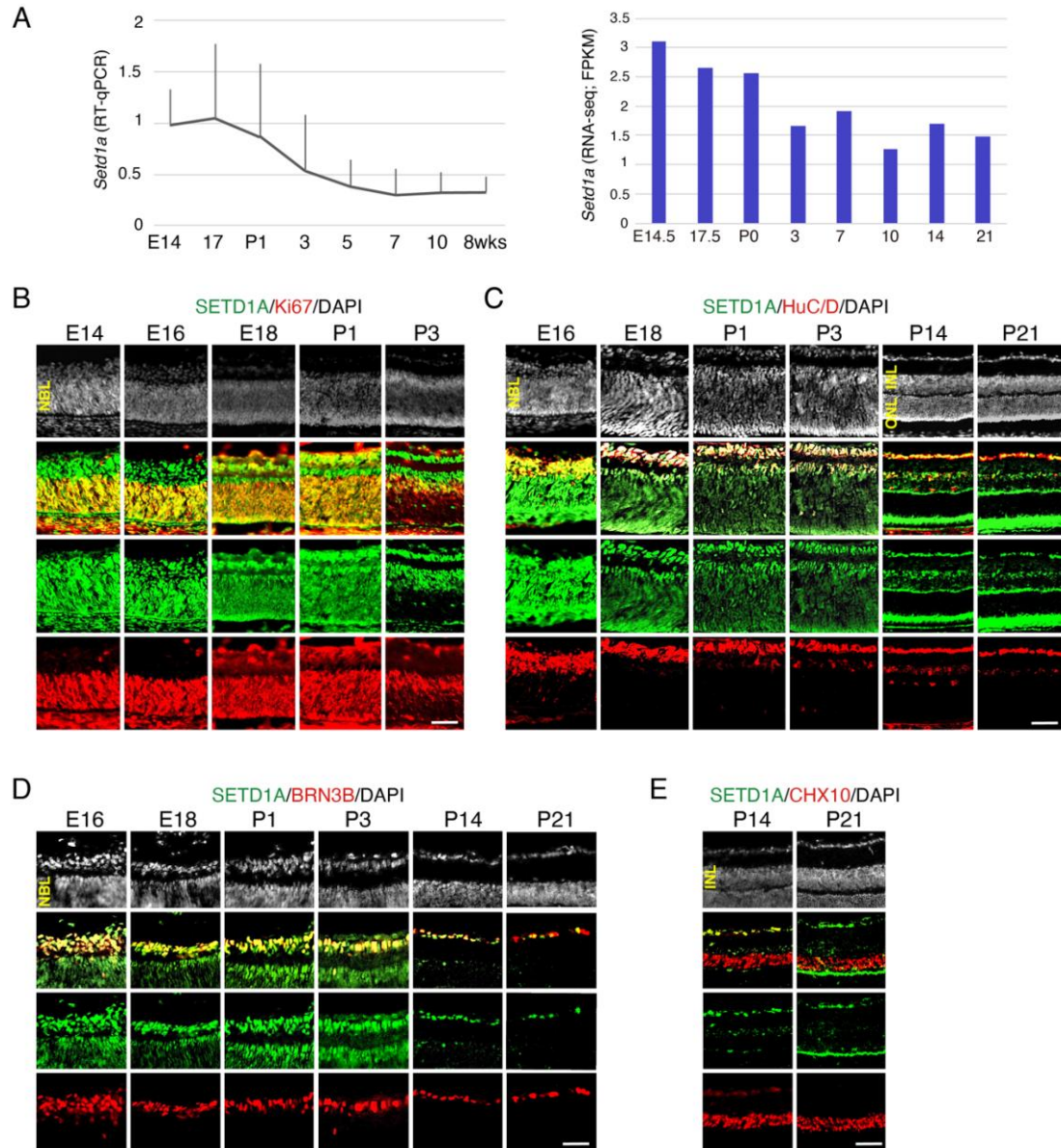


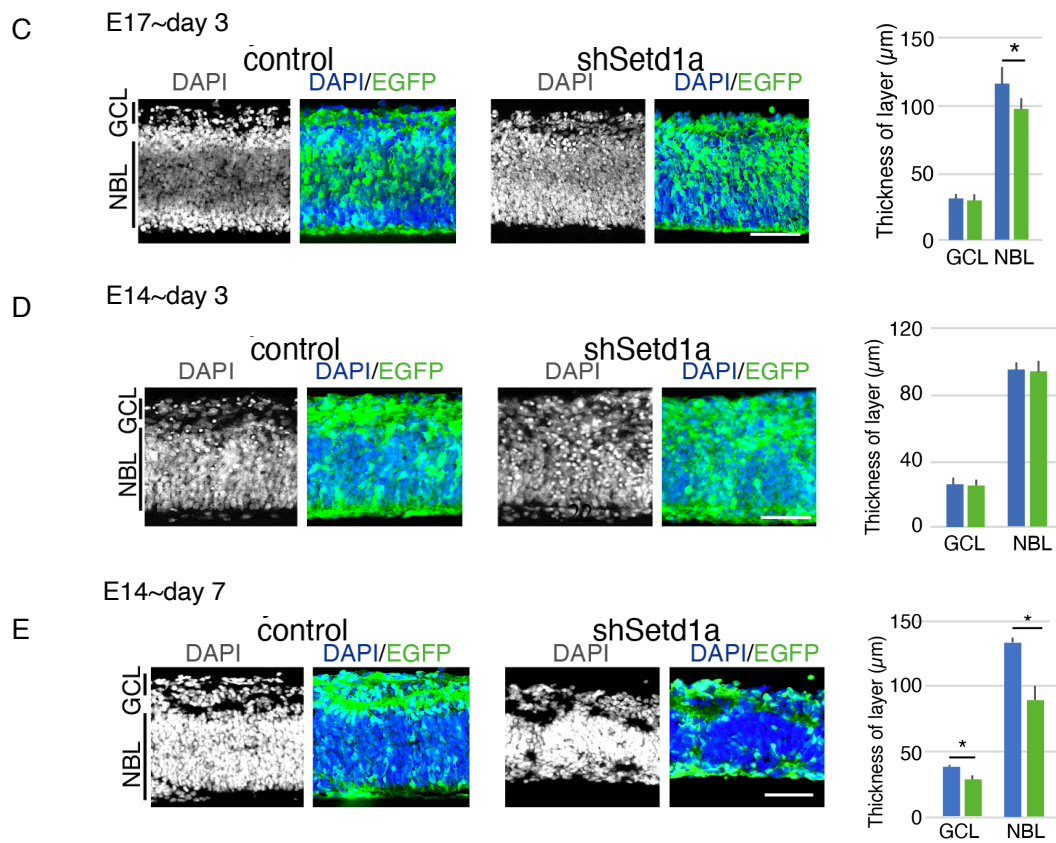
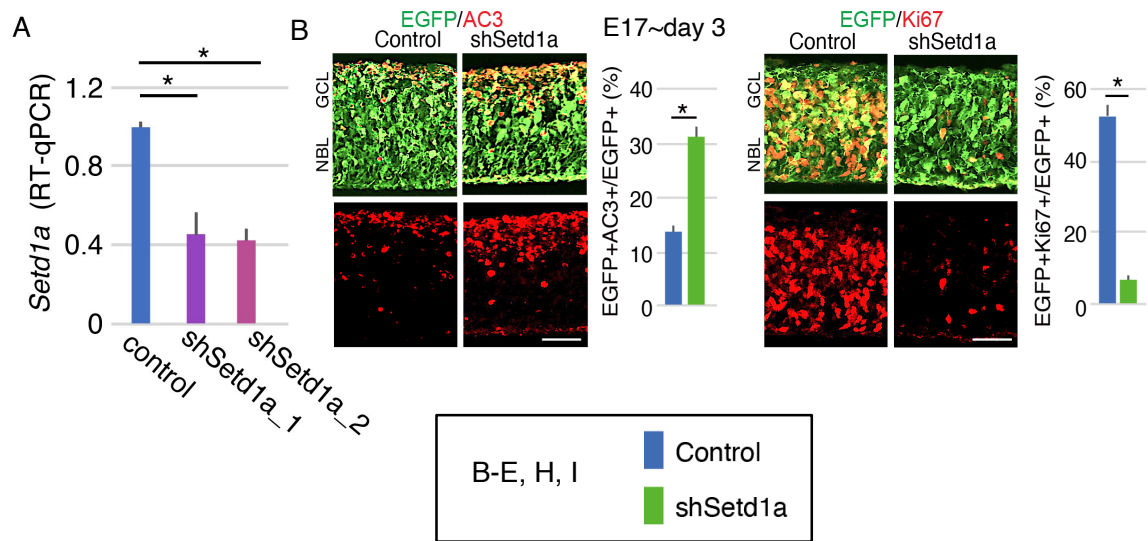
Figure 5 Transition of expression levels of *Setd1a* during retinal development

A. Transition of expression level of transcripts of *Setd1a* during mouse retinal development was examined by RT-qPCR (left panel) and RNA-Seq analysis (right panel) of developing mouse retinas (GSE87064). Left panel; Mouse whole retinas at indicated developmental stages were isolated, and RT-qPCR was performed. Relative expression levels of *Setd1a* to *Actb* and *Gapdh* are shown. The values are average of 3 independent samples with standard deviation. Right panel; fragments per kilobase of exon per million reads mapped (FPKM) value of RNA-Seq data. B-E. Expression pattern of SETD1A protein in developing retinal cells was examined by immunohistochemistry. Mouse retinas at indicated developmental stages were frozen sectioned, and immunostaining by using indicated antibodies was performed. Nuclei were visualized by staining with DAPI. NBL, neuroblastic layer; INL, inner nuclear layer; ONL, outer nuclear layer. Scale bar = 50 μ m.

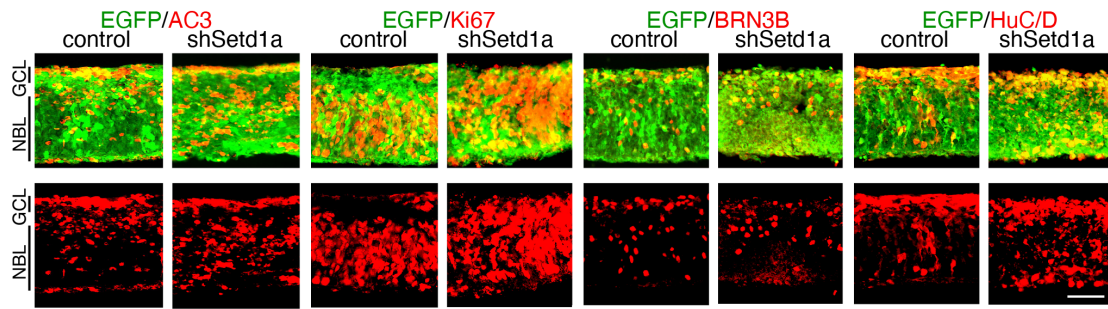
2. Downregulation of *Setd1a* expression led to apoptosis and suppressed RPC proliferation in developing retinas

To elucidate the roles of *Setd1a* in retinal development, we examined the effects of shRNA-mediated downregulation of *Setd1a* during retinal development using retinal explant culture, which mimics retinal development in an *in vitro* tissue culture system. We electroporated plasmids encoding shSetd1a or control with EGFP-expressing plasmids into isolated mouse retinas on E17, and the retinas were cultured for 3 days as explants and then harvested. Significant reduction of *Setd1a* expression in retinal explant was confirmed by RT-qPCR (Fig. 6A). Apoptosis and proliferation were examined by staining cells with anti-active Caspase 3 (AC3) and anti-Ki67 antibodies, which mark apoptotic and proliferative cells, respectively. We found that the downregulation of *Setd1a* led to an increase in apoptotic cells and a dramatic decrease in proliferating cells (Fig. 6B). The thickness of the neuroblast layer (NBL), but not that of the GCL, decreased in shSetd1a-expressing retinas (Fig. 6C).

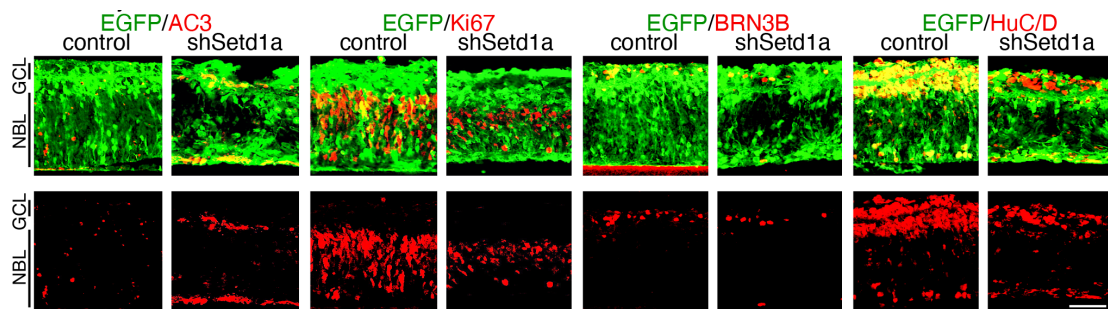
We then examined whether the downregulation of *Setd1a* exerted similar effects on RPCs at earlier stages. EGFP-expressing and shSetd1a-encoding plasmids were electroporated into isolated retinas on E14, and the retinas were cultured for 3 days as explants. The expression of shSetd1a did not affect retinal thickness (Fig. 6D). In addition, *Setd1a* depletion did not affect the abundance of apoptotic and proliferating cells. Examination of retinal ganglion cells (RGCs) and amacrine cells in early-stage retinas revealed that cell numbers did not differ between control and shSetd1a-expressing retinas (Fig. 6F, H). When the retinas were cultured for 7 days, we observed thinner NBL and GCL in shSetd1a-expressing retina (Fig. 6E). Accordingly, an increase in apoptotic cells and a decrease in proliferating cells were observed, implying that *Setd1a* depletion affects the survival and proliferation of late RPCs. Furthermore, in later stage retinas, the number of RGCs labeled by Brn3b and amacrine cells labeled by HuC/D decreased (Fig. 6G, I).



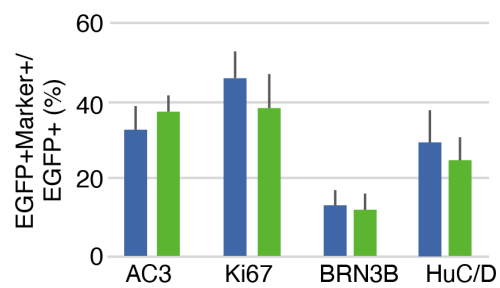
F E14~day3



G E14~day7



H E14~day 3



I E14~day 7

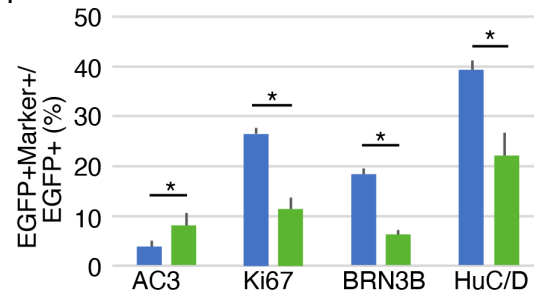


Figure 6 Downregulation of *Setd1a* expression led to apoptosis and suppressed RPC proliferation in developing retinas

Plasmids encoding control or shSetd1a, in combination with EGFP expression plasmids were electroporated into the retina derived from E17 (A-C) or E14 (D-I) embryos, and retinas were harvested after 3 days (A-D, F, H) or 7 days (E, G, I) of explant culture. After sorting EGFP-positive cells, total RNA was purified and served to RT-qPCR (A). Immunohistochemistry was done by using anti-GFP, -active Caspase 3 (AC3) antibody to detect apoptotic cells or anti-Ki67, proliferation antigen, antibody (B, F, G). Differentiation to RGC and amacrine cell were examined by staining with anti-BRN3B and -HuC/D antibodies, respectively (F, G). Populations of AC3, Ki67, BRN3B, or HuC/D and EGFP double-positive cells in total EGFP-positive cells are shown in B, H, and I. Thickness of GCL and NBL were measured (C-E). Values are average of at least 3 independent samples with standard deviation. $*p<0.05$ (Student's t-test). Scale bar = 50 μ m. GCL, ganglion cell layer; NBL, neuroblastic layer.

3. Effects of shSetd1a on the differentiation of late-stage retinal cells

The effects of shSetd1a on retinal differentiation were examined. Mouse retinas at E17 were transfected with control or shSetd1a plasmids with EGFP-expressing plasmids and cultured for 14 days as explants. Before they were harvested, the cultured retinas were observed under a bright-field microscope from the ONL side. In shSetd1a-expressing retinas, there were numerous black dots and almost no EGFP-positive cells (Fig. 7A). Examination of frozen sections confirmed that there were only a few EGFP-positive cells in shSetd1a-expressing retinas, in contrast to control retinas, in which numerous EGFP-positive cells were observed (Fig. 7A, bottom panels). The results indicated that most of the shSetd1a-expressing cells had probably disappeared via apoptosis during the culture period. We then examined whether there were differences in the abundances of specific retinal cell subtypes. Numbers of TFAP2A-positive amacrine cells were similar between control and shSetd1a-expressing retinas (Fig. 7B, C), whereas there were fewer CHX10-positive bipolar cells, cyclinD3-positive Müller glia, and PNR-positive rod photoreceptors in shSetd1a-expressing retinas (Fig. 7B, C). The latter three cell subtypes develop during the middle-to-late period of retinal development, implying that *Setd1a* depletion damages late retinal progenitors and decreases the abundance of late-stage retinal cells.

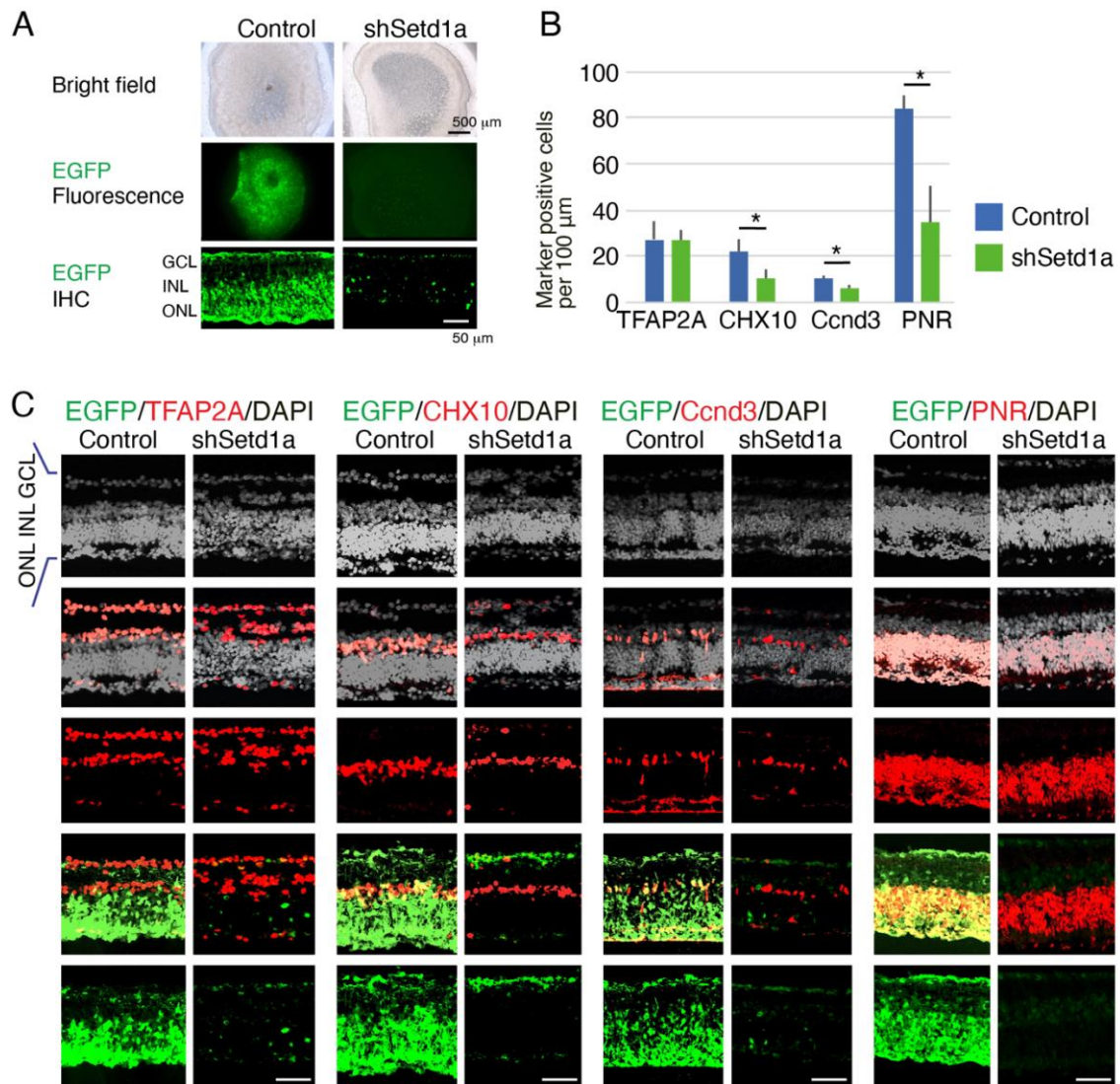


Figure 7 shRNA-mediated *Setd1a* depletion affected differentiation of late-born retinal subtypes

Retinas from E17 embryos were transfected with control- or shSetd1a- together with EGFP-expression plasmids and cultured as explants for 14 days. A. Bright field (upper panels) and fluorescent (second panels) photos taken from ONL side are shown. Bottom panels in A show immunostained frozen sections with anti-GFP antibody. B, C. Co-immunostaining using antibodies anti-GFP and -TFAP2A for amacrine cell, -CHX10 for bipolar cell, -CyclinD3 for Müller glia, or -PNR for rod photoreceptors was performed. The numbers of subtype specific protein positive cells in 100 μm vision are shown in B. Nuclei were visualized by DAPI staining in C. Values are average of at least 3 independent samples with standard deviation. * $p < 0.05$ (Student's t-test). Scale bar in black= 500 μm and white= 50 μm (A). GCL, ganglion cell layer; INL, inner nuclear layer; ONL, outer nuclear layer.

4. The SET domain is essential for the prevention of apoptosis and induction of proliferation by *Setd1a* in retinal development

We investigated whether the shSetd1a-induced phenotype was caused by *Setd1a* depletion by performing *Setd1a* complementation experiments. We first confirmed that ectopic expression of full-length SETD1A (Fig. 8A) in retinal explants did not lead to changes in the numbers of AC3-positive apoptotic cells and Ki67-positive proliferating cells (Fig. 8B–D). Then, shSetd1a and full-length SETD1A were co-transfected into retinas on E17 and cultured for 3 days. SETD1A expression reversed the increase in AC3-positive cell abundance and the decrease in Ki67-positive proliferating cell abundance (Fig. 8B–D).

The SET domain is localized at the SETD1A C-terminus (Fig. 8A) and is responsible for catalyzing H3K4me3 [49]. To determine whether the prevention of apoptosis and promotion of proliferation in RPCs by *Setd1a* were mediated by SETD1A catalytic activity, rescue experiments in which shSetd1a-expressing retinas were treated with mutant SETD1A that lacked the SET domain (SETD1A Δ SET; Fig. 8A) were performed. Co-transfection of SETD1A Δ SET with shSetd1a did not rescue apoptosis and proliferation failure (Fig. 8B–D), indicating that *Setd1a* exerts effects on retinas as observed in earlier experiments through its methyltransferase activity.

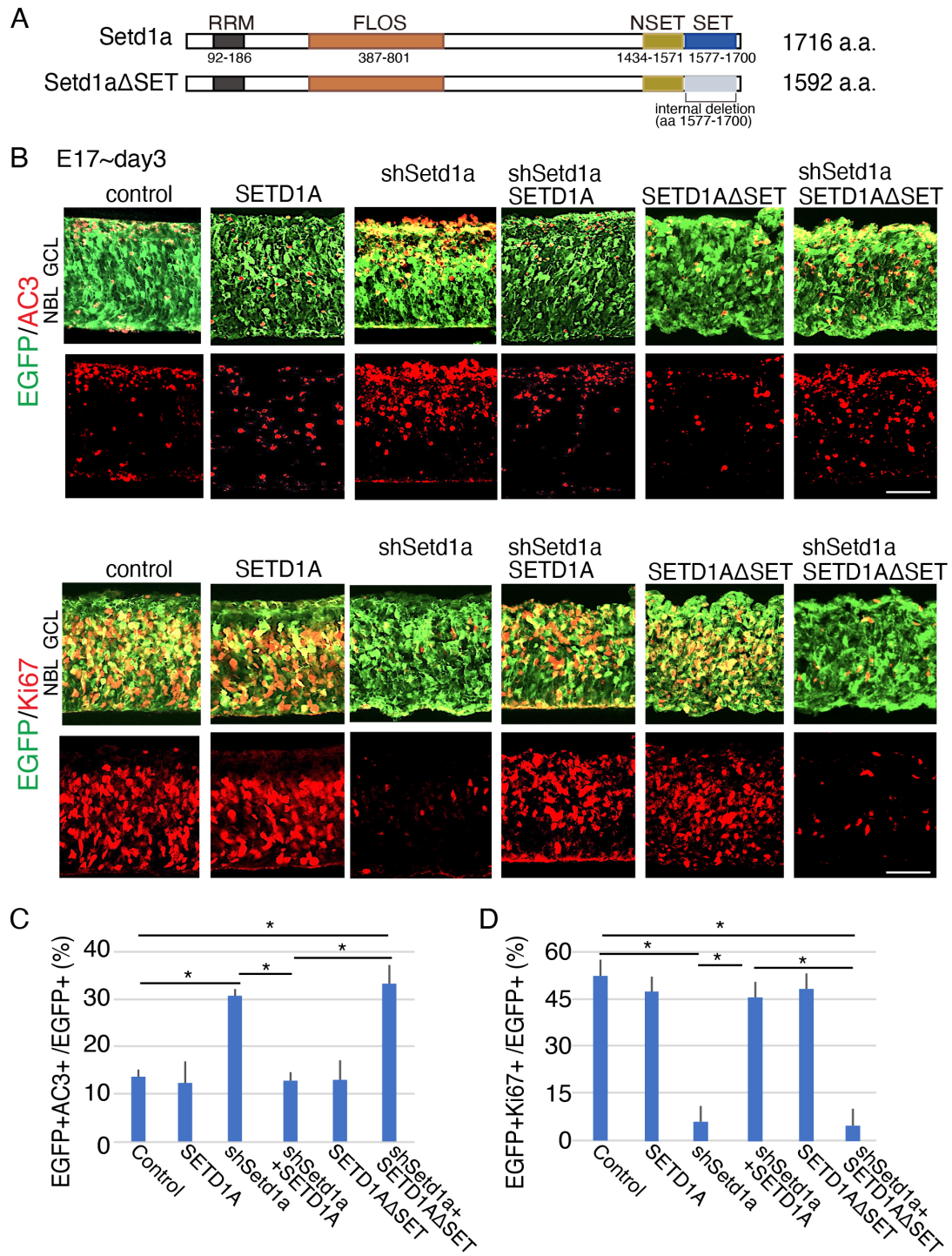


Figure 8 SET domain is essential for the function of *Setd1a* in retinal development

A. Schematic representation of SETD1A and SETD1A Δ SET (SET domain deleted SETD1A). RRM, RNA recognition motif domain; FLOS, Functional Location on SETD1A; NSET, a region near SET; SET, Su(var)-3-9, Enhancer-of-zeste, Trithorax. B-D. Plasmids encoding control, SETD1A, shSetd1a, or SETD1A Δ SET and EGFP expression plasmids were transfected as indicated into the retinas from embryos at E17, and the explant retinas were cultured for 3 days. Immunostaining was done by using anti-AC3 or -Ki67 with-GFP antibodies (B). The percentages of AC3 and EGFP (C), Ki67 and EGFP (D) double-positive cells in total EGFP-positive cells are shown. Values are average of at least 3 independent samples with standard deviation. * $p < 0.05$ (Tukey's HSD test). Scale bar = 50 μ m. GCL, ganglion cell layer; NBL, neuroblastic layer.

5. Identification of *Setd1a* target gene(s) during retinal development using RNA-Seq

RNA-Seq was performed to investigate the molecular pathways downstream of *Setd1a* activity in the retina. Plasmids encoding shSetd1a or control with an EGFP expression vector were electroporated into E17 retina, and the retinas were cultured for 2 days. EGFP-positive cells were collected via cell-sorting and subjected to RNA-Seq analysis. The gross pattern of changes in gene expression was visualized using a volcano plot (Fig. 9A), and there were similar numbers of negatively and positively regulated genes. Genes that were significantly downregulated and upregulated by shSetd1a were selected for further analyses (Fig. 9B). Initially, we searched for protein-coding genes with a transcripts-per-million value of more than 10. Of these, we selected the genes that were downregulated or upregulated by more than 50% compared to the control (Fig. 9B). Gene ontology analysis of the down-regulated 62 genes showed that the top three categories were related to cell proliferation (Fig. 9B). Conversely, according to DAVID ontology analysis, the upregulated genes were assigned to different terms (Fig. 9B). The H3K4me3 levels of the down-regulated 62 gene loci were examined by using public ChIP-Seq data of H3K4me3 in the P1 mouse retina (GSE87064) [67]. Of those genes, protein-coding genes and genes associated with H3K4me3 enrichment around the promoter region were selected. Then, genes localized on the XY chromosomes were excluded, and only genes with a peak q score [$-10 \times \log(q\text{-value})$] of more than 400 were retained. Among the remaining 4976 genes, 17 genes overlapped with the 62 genes identified via RNA-Seq (Fig. 9C, D). Most of the genes detected were associated with cell proliferation (Table 1), consistent with the results of DAVID ontology analysis. Among those genes, we chose *Uhrfl* as a candidate target gene of *Setd1a*, because UHRF1 was reported to form a complex with SETD1A and maintain bivalent histone marks at cell specification-associated domains in embryonic stem cells (ESCs) [35].

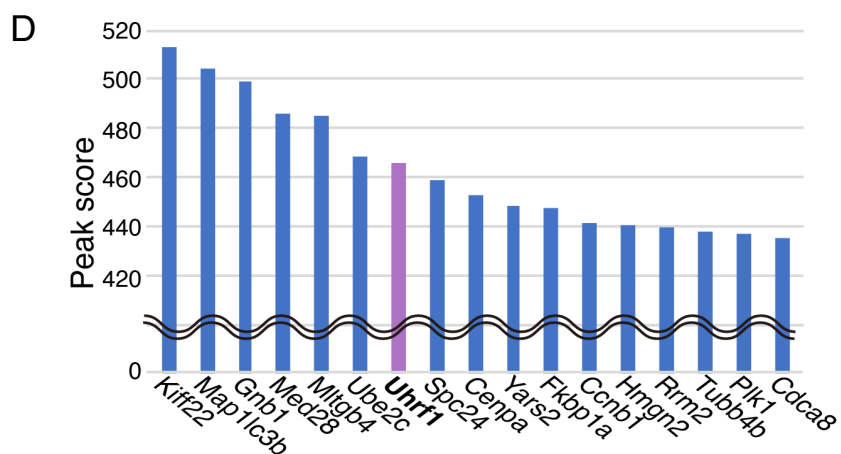
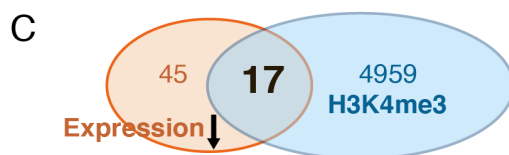
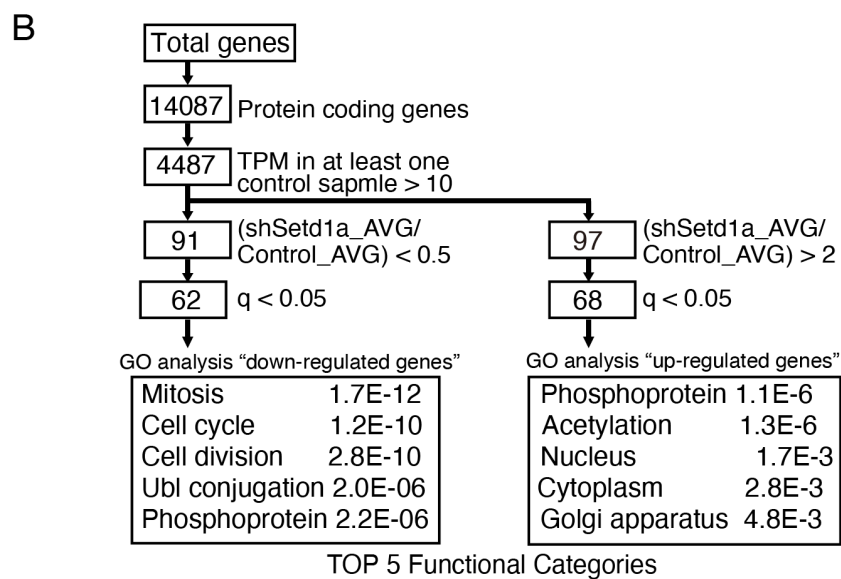
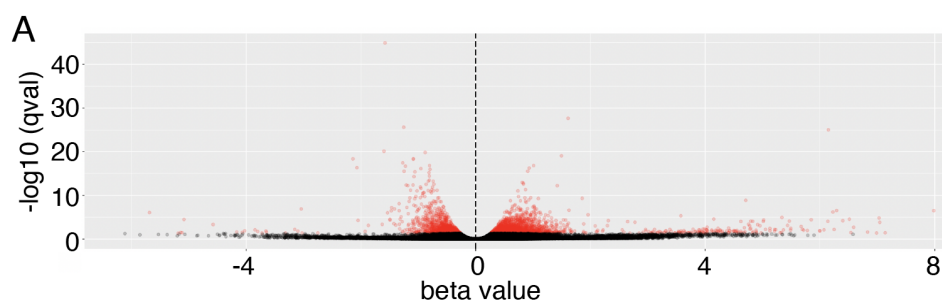


Figure 9 Identification of *Setd1a* target gene(s) during retinal development using RNA-Seq and ChIP-seq

Plasmids encoding control or shSetd1a were co-transfected with EGFP expression vector into retina from E17 embryos, and the retinas were cultured as the explants for 2 days. Total RNA was purified and served to RNA-Seq. Distribution of IDs are shown as a volcano plot in A. Q-value is plotted in the vertical axis indicates, and beta value (natural log fold change) is plotted on the horizontal axis. Schematic diagram of the flow of analyses. Both down- and up-regulated genes were subjected to DAVID for gene ontology analysis. Top five functional categories of 62 and 68 genes are shown in B. C. Relation of the down-regulated 62 genes from RNA-Seq analysis and 4976 genes with high enrichment of H3K4me3 selected from ChIP-seq data (GSE87064, Aldiri, Neuron 94, 550-568, 2017) was examined and shown as Venn diagram. D. Peak score of the 17 genes in the Venn diagram (C) is shown. Highlighted 17 genes from the top peak scores are shown from the left.

Table 1 Most of the 17 genes detected were associated with cell proliferation

Gene_Name	Functions	REF.1	REF.2
<i>Kif22</i>	Cancer cell proliferation; ATPase activity and microtubule motor activity	Yu Y et al. Carcinogenesis. 2014	Pike R et al. Sci Signal. 2018
<i>Map1lc3b</i>	Cell proliferation; Tumor invasion; Inflammatory state of the retina	Liu PF et al. J Clin Med. 2018	Dhingra et al. Front Cell Neurosci. 2018
<i>Gnb1</i>	Rod transducin subunit; GTPase activity; Located photoreceptor segments	Lohmann et al. Hum Mol Genet. 2017	Petrovski et al. Am J Hum Genet. 2016
<i>Med28</i>	Cell proliferation; Upregulated in cancer stem cell; Pluripotency of the inner cell mass	Cho et al. Oncol Lett. 2018	Li et al. PLoS One. 2015
<i>Itgb5</i>	Fibroblasts proliferation; Proliferation of breast and cervical cancer cells	Wang et al. Am J Cancer Res. 2016	Conway et al. Cell Rep. 2016
<i>Ube2c</i>	Oncogene by enhancing cell proliferation, migration, invasion; A ubiquitin ligase that controls progression through mitosis	Xiong et al. Biosci Rep. 2019	Liu et al. Mol Cancer Res. 2020
<i>Uhrf1</i>	G1/S transition; DNA methylation and chromatin modification; Required for development and maintenance of the zebrafish lens; Highly expressed in retinoblastoma;	Patnaik et al. Oncotarget. 2018	Tittle et al. Dev Biol. 2011
<i>Spc24</i>	Chromosome segregation and kinetochore integrity; Cell cycle, Mitotic; Regulate some cancers progression	Ma et al. Mol Biol Cell. 2007	Zhu et al. Oncotarget. 2015
<i>Cenpa</i>	Found in centromeric nucleosomes; An epigenetic mark in replication and cell division; Cancer formation	Quénet et al. Chromosome Res. 2012	Black et al. Cell. 2011
<i>Yars2</i>	Related to nucleotide binding, tRNA binding; Mutations cause some kinds of anemia	Zhang et al. J Cancer Res Clin Oncol. 2020	Fujiwara et al. Pediatr Int. 2013
<i>Fkbp1a</i>	Mediates necroptosis; Involved in proliferation in a Rat Model of Endometriosis	Seguinot et al. Reprod Sci. 2020	Terukina et al. Dev Growth Differ. 2011
<i>Ccnb1</i>	Key cell cycle activator, control the G2/M transition phase; Downregulation affect retinal pigmented epithelial cell proliferation	Farshadi et al. Cell Cycle. 2019	Barton et al. Dev Dyn. 2008
<i>Hmgn2</i>	Chromatin Regulation; Acetylation; Nucleosomal DNA binding	Garza et al. Epigenetics & Chromatin. 2019	Fan et al. Oncol Lett. 2019
<i>Rrm2</i>	Provides the precursors necessary for DNA synthesis; G1/S transition; Upregulated in retinoblastoma	Chen et al. Nat Commun. 2019	Nie C et al. Ophthalmologica. 2020
<i>Tubb4b</i>	Major constituent of microtubules; Spindle assembly and chromosome separation; Mutations cause Leber congenital amaurosis (LCA)	Laskowski et al. Theriogenology. 2017	Luscan et al. Am J Hum Genet. 2017
<i>Plk1</i>	Depletion in cancer cells inhibite cell proliferation and induced apoptosis; M phase	De Blasio C et al. J Biol Chem. 2019	Gao et al. Cancer Gene Ther. 2020
<i>Cdca8</i>	Microtubule stabilization and spindle formation; Knockdown inhibits the proliferation and enhances the apoptosis of cancer cells	Gao X et al. PeerJ. 2020	Sampath et al. Cell. 2004

Gene name were listed in the order of peak score. Main functions and typical researches of genes were shown as reference 1, 2.

6. H3K4me3 level at the *Uhrfl* locus is modulated by *Setd1a* expression level

The expression pattern of *Uhrfl* transcripts (Fig. 10A) during retinal development was analyzed based on RNA-Seq data on developing mouse retinas (GSE87064). Expression levels of *Uhrfl* transcripts were highest in E14.5 embryonic retinas, then decreased continuously through the rest of retinal development (Fig. 10B). Our RNA-Seq analysis of shSetd1a showed that the expression levels of *Uhrfl* variants 204 and 207 (Fig. 10A) were significantly lower in shSetd1a-expressing retinas than in control retinas. The expression level of variant 203 also decreased, but the difference was not statistically significant (Fig. 10C). The other two forms, which use the first exon as the start site, were expressed very weakly, and no significant differences were observed between shSetd1a-expressing and control retinas (Fig. 10C). According to publicly available online data (viz.stjude.cloud, [67]), two H3K4me3 peaks are associated with the *Uhrfl* locus, around the transcriptional start sites of the first and second exons (Fig. 10D). The association between H3K4me3 and the *Uhrfl* locus was examined via ChIP-qPCR using three primer sets—one for the weakly methylated 5' region, and two for methylation peaks (Fig. 10D). Plasmids encoding shSetd1a or control with an EGFP expression vector were electroporated into E17 retina, and the retinas were cultured for 2 days. EGFP-positive cells were sorted using a cell sorter and subjected to ChIP-qPCR. Signal levels from reactions using primer C, which amplifies the region around the H3K4me3 peak at the 3' side, were significantly lower in shSetd1a-expressing retina (Fig. 10E), which is consistent with the lower transcript levels of *Uhrfl* variants 204 and 207 in shSetd1a-expressing retinas (Fig. 10C).

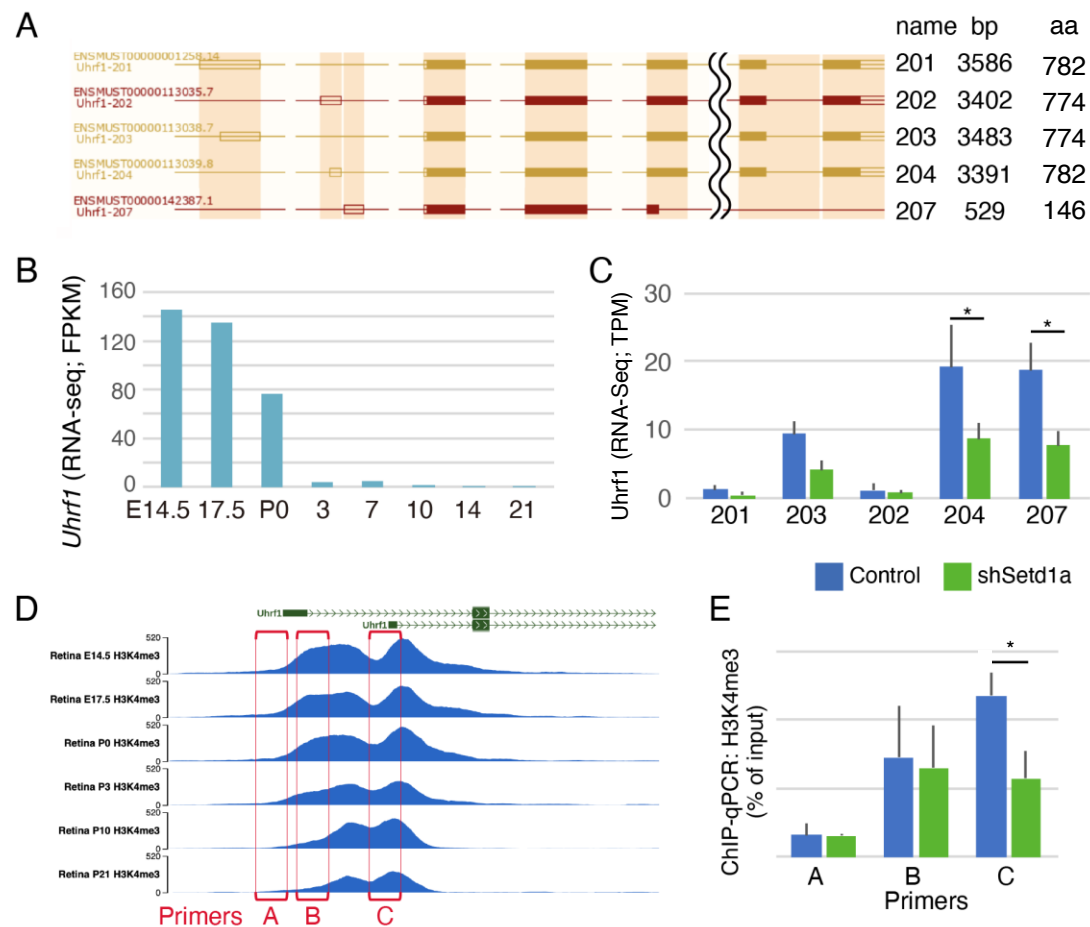


Figure 10 Expression of *Uhrf1* transcripts was decreased by the expression of shSetd1a

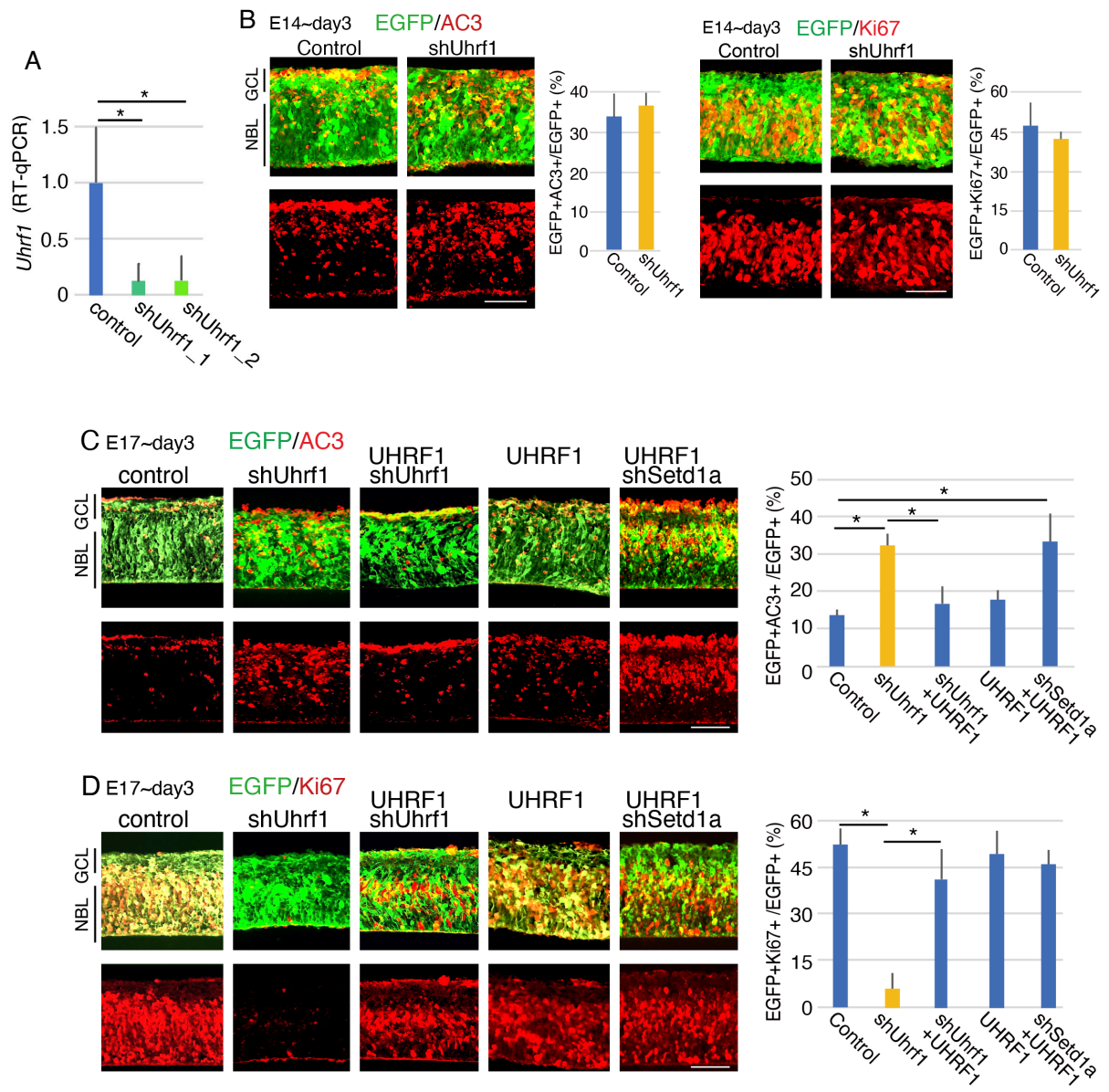
A. Schematic representation of alternative splicing products of *Uhrf1*. Adapted from the schematic data of asia.ensembl.org. B. Transition of expression level of transcripts of *Uhrf1* during mouse retinal development from RNA-Seq data of whole mouse retina (GSE87064)[67]. C. Retinas at E17 were transfected with control or shSetd1a plasmids with an EGFP expression vector and cultured for 2 days. EGFP positive-cells were purified, and RNA-Seq was performed. Expression levels of *Uhrf1* splicing variants in the control or shSetd1a-expressing retinas are shown. Values are average of 4 samples of both control and shSetd1a RNA-Seq (GSE154498) data with standard deviation. * $q < 0.05$ (false discovery rate). TPM, Transcripts per million. D. H3K4me3 levels at *Uhrf1* locus during mouse retinal development from ChIP-Seq data of whole mouse retina (viz.stjude.cloud, [67]). Locus of three primer sets for ChIP-qPCR (E) are shown in red box. E. The retinas at E17 were transfected with control or shSetd1a with EGFP expression plasmids and cultured for 2 days. Then, the retinas were subjected to ChIP-qPCR using anti-H3K4me3 antibody. *Uhrf1* promoter regions were amplified by using 3 different primer sets. Values are average of at least 3 independent samples with standard deviation. * $p < 0.05$ (Student's t-test).

7. *Uhrfl* knockdown resulted in increased apoptosis and proliferation failure in RPCs

We next examined the effects of *Uhrfl* knockdown on retinal development. The *Uhrfl* expression was significantly decreased in the explant retina expressing shUhrfl (Fig. 11A). We transfected shUhrfl-encoding plasmids with an EGFP expression vector into isolated mouse retinas on E14 and harvested the retinas after 3 days of explant culture. Numbers of AC3-positive cells were almost the same between control and shUhrfl-expressing retinas, and the abundance of Ki67-positive proliferating cells also did not differ between control and shUhrfl-expressing retinal cells (Fig. 11B). We then transfected shUhrfl and EGFP expression plasmids into retinas on E17 and cultured the retinas for 3 days. The abundance of AC3-positive apoptotic cells increased dramatically (Fig. 11C), and Ki67-positive proliferating cells nearly disappeared (Fig. 11D).

To examine the effects of *Uhrfl* loss-of-function on retinal cell differentiation, we extended the culture period for retinal explants to 14 days. TFAP2A-positive amacrine cells were not affected, but the numbers of CHX10-positive bipolar cells, cyclinD3-positive Müller glia, and PNR-positive rod photoreceptors decreased in shUhrfl-expressing retinas (Fig. 11E, F).

Upon co-transfection of full-length *Uhrfl* and shUhrfl expression plasmids, the increase in apoptotic cells and decrease in proliferating cells induced by *Uhrfl* depletion were reversed (Fig. 11C, D). The expression of full-length UHRF1 alone did not affect apoptosis and proliferation in the retina (Fig. 11C, D). Finally, to determine whether ectopic expression of UHRF1 reverses the shSetd1a-induced phenotype, UHRF1 was co-expressed with shSetd1a. Co-expression led to an increase in apoptotic cells, but UHRF1 expression reversed the shSetd1a-induced inhibition of proliferation (Fig. 11C, D), implying that apoptosis and proliferation are regulated by different mechanisms.



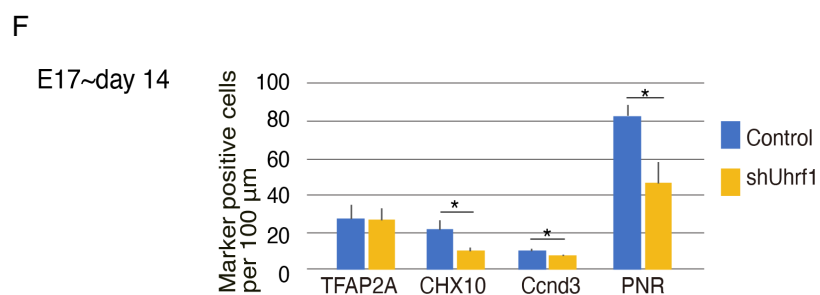
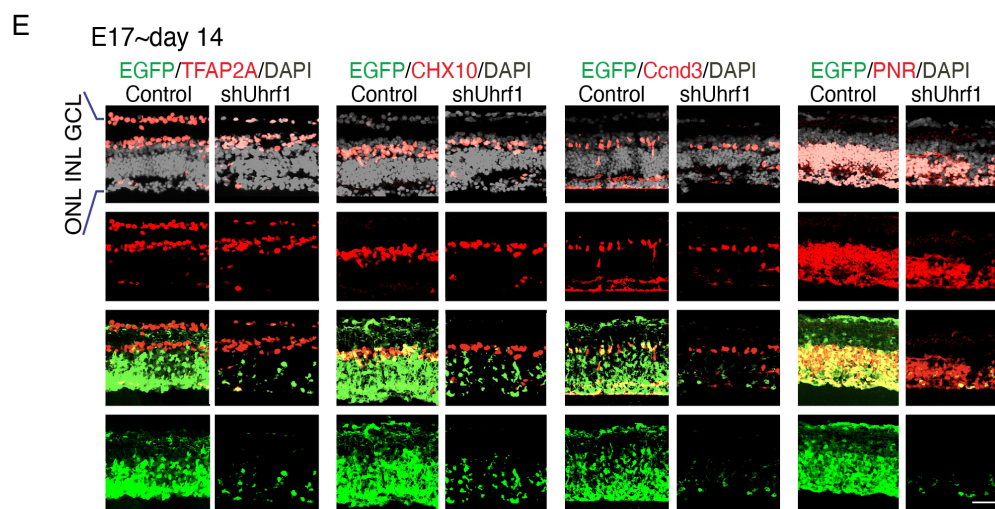


Figure 11 Expression of shUhrf1 perturbed retinal development

Control, shUhrf1_1, shUhrf1_2 with EGFP expression plasmid were transfected to the isolated retinas at E17, and the retinas were culture for 3 days. After sorting EGFP-positive cells, total RNA was purified and served to RT-qPCR (A). Plasmids encoding control, shUhrf1, UHRF1, or shSetd1a and EGFP expression plasmids were electroporated into mouse retina at E14 (B) or E17 (C-F). Combination of transfected plasmids are indicated in the figures. The retinas were then cultured for 3 (B-D) or 14 days (E, F) and frozen sectioned. Immunostaining using anti-AC3 or anti-Ki67 with -EGFP antibodies was done. The percentages of EGFP and AC3 or EGFP and Ki67 double-positive cells in the total EGFP-positive cells are shown (B-D). Co-immunostaining using antibodies anti-GFP and -TFAP2A for amacrine cell, -CHX10 for bipolar cell, -CyclinD3 for Müller glia, or -PNR for rod photoreceptors was performed (E). The numbers of subtype specific protein positive cells in 100 μ m vision are shown in F. Nuclei were visualized by DAPI staining in E. Values are average of 3 independent samples with standard deviation. * $p < 0.05$ (Tukey's HSD test in C, D; Student's t-test in F). Scale bar = 50 μ m. GCL, ganglion cell layer; NBL, neuroblastic layer; INL, inner nuclear layer; ONL, outer nuclear layer.

8. *Uhrf1* depletion did not lead to changes in bulk DNA methylation in the retina

Uhrf1 is a hemi-methylated DNA-binding protein and facilitates DNA methylation by recruiting *Dnmt1* [73]–[75]. We investigated whether loss of *Uhrf1* contributes to global DNA hypomethylation in the retina by immunostaining to detect 5-methylcytosine (5mC). Plasmids encoding shUhrf1 with an EGFP-expressing vector were transfected into isolated retinas on E17, and the retinas were harvested after 3 days. Because apoptotic cells can create noise in the background with 5mC staining [76], shUhrf1-expressing retinas were cultured with ZVAD, an apoptosis inhibitor [77]. No AC3-positive apoptotic cells were observed after treatment with ZVAD (Fig. 12A). Then, retinal sections were stained with the anti-5mC antibody. The 5mC signal intensities did not differ between ZVAD-treated control and shUhrf1-expressing cells (Fig. 12B). For the control experiment, retinas were treated with 1 μ M 5-Aza (A3656; Sigma-Aldrich), an inhibitor of DNMT1 that lead to DNA hypomethylation. After 3 days, the retinas were frozen and sectioned. At 1 μ M of 5-Aza, proliferation was only slightly suppressed, and the number of apoptotic cells increased slightly (Fig. 12C). Additionally, 5mC signal intensities appeared to decrease in the presence of 5-Aza (Fig. 12C), indicating that the antibody could detect the decrease in DNA methylation level.

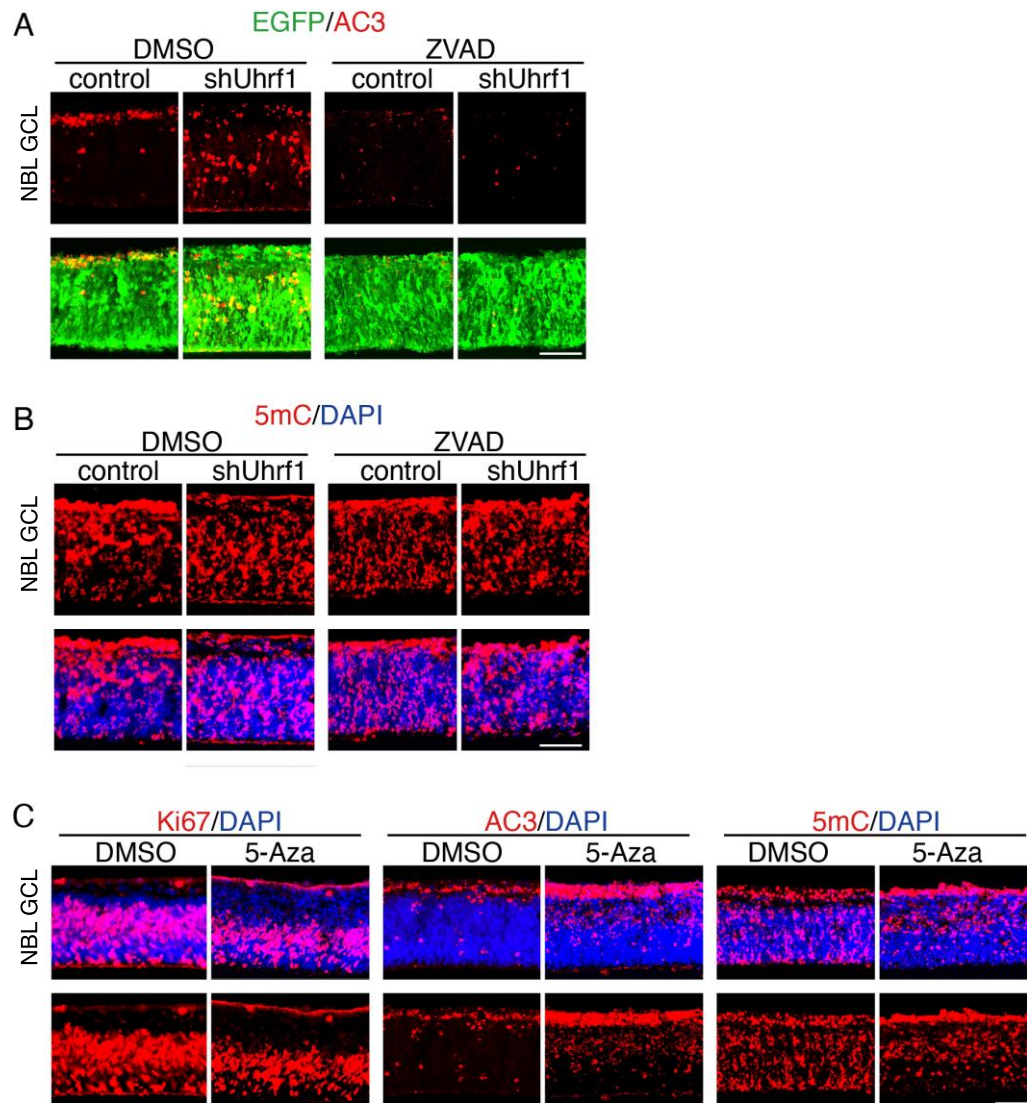


Figure 12 *Uhrf1* depletion did not lead to changes in bulk DNA methylation in the retina. Plasmids encoding shUhrf1 with an EGFP-expressing vector were transfected into isolated retinas on E17, and the retinas were cultured with 20 μ M ZVAD for 3 days (A, B). Immunostaining using anti-AC3 with -EGFP antibodies (A), or anti-5mC (B) was done. Retinas were treated with 1 μ M 5-Aza and after 3-day culture, the retinas were frozen and sectioned (C). Immunostaining by anti-Ki67, anti-AC3, or anti-5mC was performed. Nuclei were visualized by DAPI staining in B and C. All conditions have been triplicated. Scale bar = 50 μ m. GCL, ganglion cell layer; NBL, neuroblastic layer.

Discussion

During retinal development, all retinal subtype neurons and glia cell are derived from RPCs, and there is an evolutionarily conserved order of genesis of the retinal subtype cells. The molecular mechanisms of epigenetic modifications that contribute to cell fate are under investigation [78]. In our previous studies, we observed reduction in amacrine cells and horizontal cells in retina specific conditional *Jmjd3* (a demethylase specific to H3K27me3) knockout mice [79]. Moreover, retina-specific *Utx* (another H3K27 demethylase) and *Jmjd3* double-knockout mice resulted in a reduced number of protein kinase C (PKC) α -positive rod ON-bipolar cells [80].

At least nine methyltransferases and five demethylases have been reported to target histone H3K4me1/2/3 as a substrate in mammals [45], [47]. H3K4 methylation is reported to be involved in rod photoreceptor development during retinal development [38], [43], [81]. Here, we investigated the roles H3K4 methylation plays in RPCs and the expression patterns of related genes using previously published RNA-Seq data [67]. We found that *Kmt2c* and *Kmt2h* are expressed from the early stages of retinal development, whereas other genes were expressed at low levels and *Setd1b/Kmt2g* at very low levels (Fig. 13). As a preliminary study, we performed mini-screening of the functions of H3K4 methylases and demethylases during early retinal development using an shRNA-mediated loss-of-function approach with retinal explant culture. We found that several shRNAs disrupted retinal development; among them, shSetd1a exerted the strongest effects, by inducing apoptosis and suppressing proliferation. Therefore, we focused on analyzing the functions of *Setd1a* during early retinal development.

Among methyltransferases, *Setd1a* exerts strong effects and performs a unique function; thus, other methylases could not compensate for the loss in function when *Setd1a* was depleted. Methylases can be divided into several subgroups according to their structure [41].

Setd1a and *Setd1b* belong to a subgroup characterized by the presence of an RRM domain [82] in addition to the FLOS region [52]. The C-terminal SET domain is found in all H3K4 methyltransferases; hence, it is possible that the RRM and/or FLOS domains contribute to SETD1A function. Although SETD1B has the same domains as SETD1A, it is unlikely that it can replace SETD1A because it is expressed at low levels (Fig. 13). In fact, the embryonic defects suggest that SETD1A functions shortly after epiblast formation but before gastrulation, while SETD1B is as well indispensable for embryonic development, but is required at a later stage. *Setd1b* knockout mice die after gastrulation between E10.5 and E11.5 [48]. To confirm in my study, although we transfected shSetd1b expression vector in addition to shSetd1a expression vector into the E14 retina, we did not observe perturbation of proliferation nor cell death of early retinal progenitors (Fig. 14).

Uhrf1 was identified as a possible downstream gene target of *Setd1a*. Because UHRF1 overexpression rescued the shSetd1a-induced suppression of proliferation, SETD1A may induce cell proliferation by inducing UHRF1. By contrast, UHRF1 expression did not reverse the induction of apoptosis in the absence of SETD1A, indicating that either the inhibition of apoptosis by SETD1A does not depend on UHRF1 or that both SETD1A and UHRF1 are necessary for the process, which is more likely because SETD1A and UHRF1 form a complex [35]. UHRF1 binds to hemi-methylated DNA to recruit DNMT1, leading to DNA methylation [20], [21], [83]. *Dnmt1* and *Dnmt3a/b* are reported to be involved in photoreceptor and outer plexiform layer development during mammalian retinal development [83], and *Dnmt1*-dependent DNA methylation is essential for photoreceptor-

terminal differentiation and retinal neuron survival [84]. We did not observe marked changes in DNA methylation in the absence of *Uhrfl*, but differences in retinal phenotypes induced by *Dnmt1* and *Uhrfl* depletion indicate that the outcomes of shUhrfl expression in the retina cannot be explained by the disruption of DNA methylation alone. *Uhrfl* is reported to be involved in regulating H3K4me3 in collaboration with *Setd1a* in ESCs [35]. UHRF1 forms a complex with SETD1A/COMPASS and regulates neuroectoderm and mesoderm differentiation [35]. We did not directly analyze the regulation of differentiation of retinal cell subtypes by SETD1A or UHRF1, but the involvement of such collaborative mechanisms in the prevention of apoptosis is feasible.

Interestingly, DAVID ontology analysis of the differentially expressed genes in shSetd1a-expressing retinas (as detected using RNA-Seq) showed that the genes were mostly associated with cell proliferation. It is known that SETD1A supported mitotic processes and its depletion lead to chromosome misalignment and segregation defects. Cell cycle arrest and senescence caused by SETD1A knockdown is independent of mutations in *p53*, *RB* and *p16*, but through suppression of SKP2 [51]. In the present study, we hypothesize that *Setd1a* enhances the transcriptional activation of proliferation-related genes through its H3K4 methyltransferase activity, and thus there are several candidate targets from the selected genes (Table 1) under our investigation for their known roles in cell proliferation. For example, *Rrm2* and *Ube2c* are positively involved in DNA replication and contribute to tumor cell growth [85], [86], and we are trying to figure out their roles in retinal development as well as their relations with *Setd1a*.

On the other hand, *Setd1a*-induced methylation and transcriptional activation may be regulated independently, as reported in yeast and flies. In *Saccharomyces cerevisiae*, SET1 methylates DAM1, a protein involved in kinetochore assembly and chromosome segregation [87], and in *S. pombe*, SET1 participates in the silencing and genome organization of retrotransposons independently of H3K4 methylation activity [88]. In *Drosophila*, H3K4A mutations abolish global H3K4 methylation but not transcriptional activity [89]. In mammals, deletion of the SET1 complex subunit CFP1 in mouse ESCs results in a global reduction of H3K4me3 in CpG island promoters. However, transcription levels did not change [90]. Although the suppression of proliferation-related genes including *Uhrf1* is a major reason explaining the loss of proliferation activity in RPCs, transcription-independent mechanisms should also be considered.

The specific deletion of *Setd1a* in adult long-term hematopoietic stem cells resulted in the loss of proliferative capacity and a failure to repair DNA damage in these cells [91]. However, according to our RNA-Seq analysis, shSetd1a did not affect expression of the genes selected for analysis. Abnormalities in the H3K4 methyltransferases *Mll1*, *Mll3*, and *Mll4* have been shown to result in cancer and hematopoietic malignancies [48]. In addition, in MLL-AF9 leukemia, SETD1A is required for cell survival and leukemia progression *in vitro* as well as *in vivo* [52]. Taken together, these findings indicate that *Setd1a* is strongly associated with cell proliferation and survival, but some tissue-specific mechanisms that regulate *Setd1a* function remain to be determined.

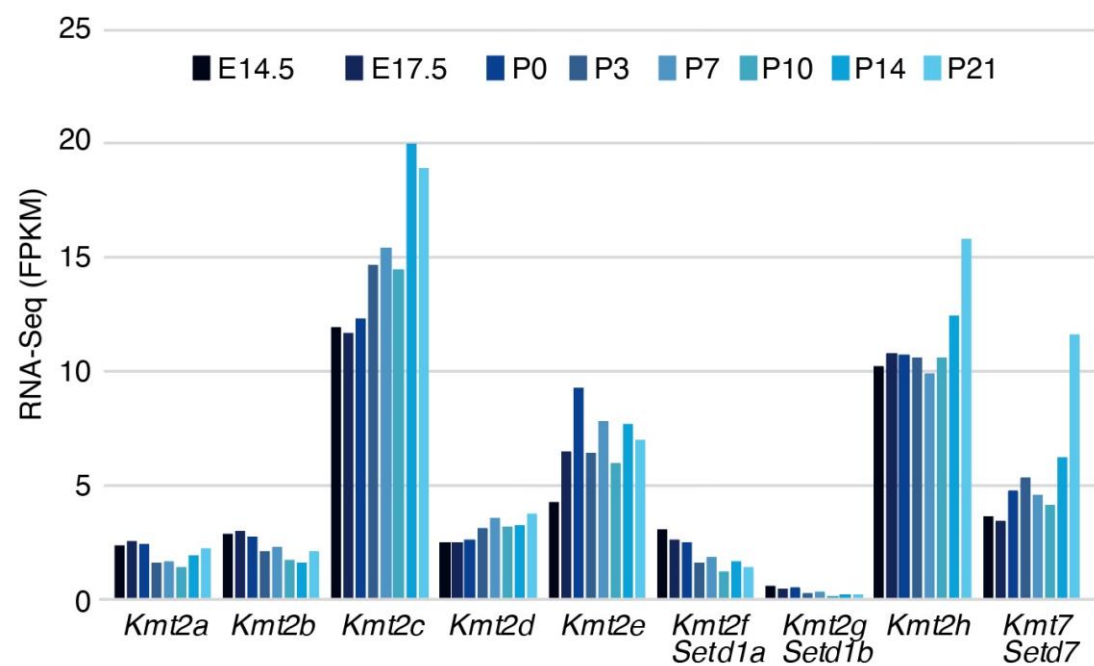


Figure 13 FPKM value of H3K4 methyltransferases by RNA-Seq during retinal development

Expression level of transcripts of KMT family members examined by RNA-Seq of whole mouse retina (GSE87064, Aldiri, Neuron 94, 550-568, 2017)

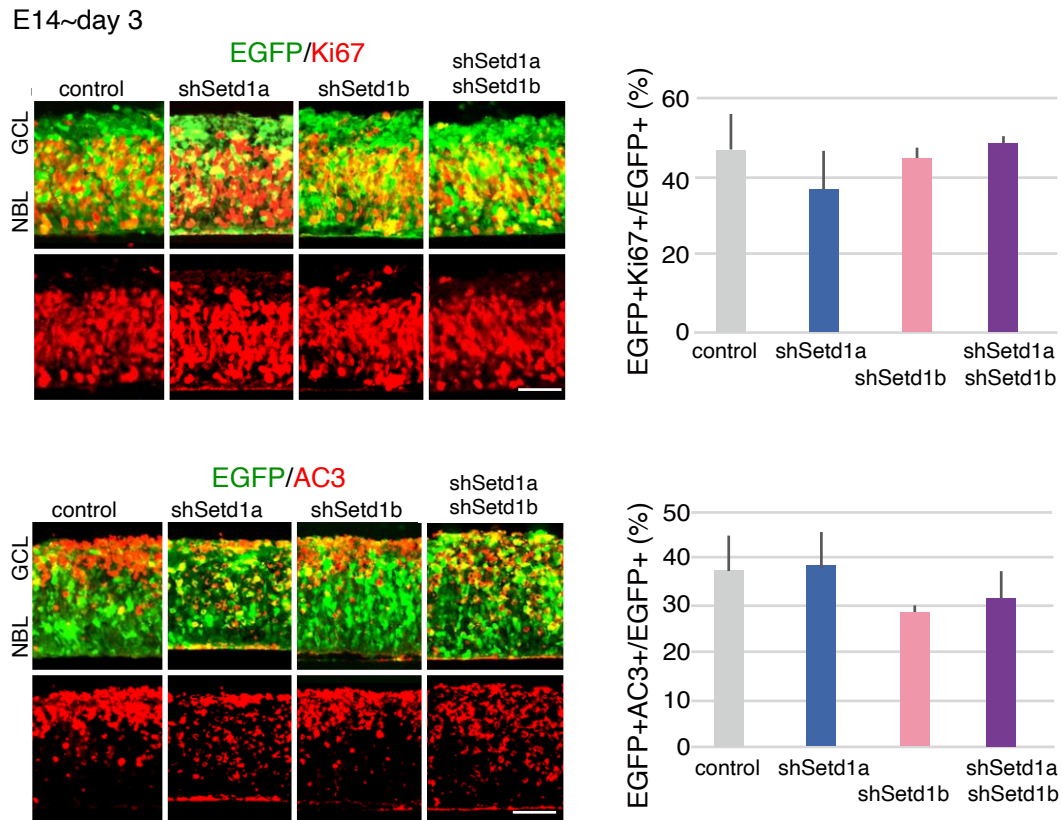


Figure 14 *Setd1b* depletion (in addition to *Setd1a* depletion) did not lead to any changes in early RPCs

Plasmids encoding control or shSetd1a, shSetd1b, in combination with EGFP expression plasmids were electroporated into the retina derived from E14 embryos, and retinas were harvested after 3 days of explant culture. Immunohistochemistry was done by using anti-GFP, -active Caspase 3 (AC3) antibody or anti-Ki67 antibody. Populations of marker and EGFP double-positive cells in total EGFP-positive cells are shown. Values are average of at least 3 independent samples with standard deviation. Scale bar = 50 μ m. GCL, ganglion cell layer; NBL, neuroblastic layer.

Conclusion

We figured out the effects of shRNA-mediated knock-down of the H3K4me3 methyltransferase *Setd1a* *in vitro* retinas, which were proliferation failure and increased apoptosis, indicating that *Setd1a* contributes to the survival and proliferation of retinal cells by regulating histone methylation. A potential downstream effector, *Uhrfl*, on proliferation and apoptosis was also functionally validated. Taken together, our results demonstrate that *Setd1a* regulates *Uhrfl* expression, and these two molecules co-operate to regulate retinal progenitor cell survival and proliferation. Though some tissue-specific mechanisms that regulate *Setd1a* function remain to be determined, *Setd1a* was proved to be strongly associated with cell proliferation and survival, which enriched the knowledge of histone modifications involved in retinal development.

References

- [1] E. A. Bassett and V. A. Wallace, "Cell fate determination in the vertebrate retina," *Trends in Neurosciences*, vol. 35, no. 9, pp. 565–573, 2012.
- [2] L. Centanin and J. Wittbrodt, "Retinal neurogenesis," *Development (Cambridge)*, vol. 141, no. 2, pp. 241–244, 2014.
- [3] R. Margueron and D. Reinberg, "The Polycomb complex PRC2 and its mark in life," *Nature*, vol. 469, no. 7330, pp. 343–349, 2011.
- [4] C. Cepko, "Intrinsically different retinal progenitor cells produce specific types of progeny," *Nature Reviews Neuroscience*, vol. 15, no. 9, pp. 615–627, 2014.
- [5] B. S. Clark, G. L. Stein-O'Brien, F. Shiau, G. H. Cannon, E. Davis-Marcisak, T. Sherman, C. P. Santiago, T. V. Hoang, F. Rajaii, R. E. James-Esposito, R. M. Gronostajski, E. J. Fertig, L. A. Goff, and S. Blackshaw, "Single-Cell RNA-Seq Analysis of Retinal Development Identifies NFI Factors as Regulating Mitotic Exit and Late-Born Cell Specification," *Neuron*, vol. 102, no. 6, pp. 1111–1126.e5, 2019.
- [6] D. M. Davis and M. A. Dyer, "Retinal progenitor cells, differentiation, and barriers to cell cycle reentry," *Current Topics in Developmental Biology*, vol. 93, no. C, pp. 175–188, 2010.
- [7] M. Xiang, "Intrinsic control of mammalian retinogenesis," *Cellular and Molecular Life Sciences*, vol. 70, no. 14, pp. 2519–2532, 2013.
- [8] A. Swaroop, D. Kim, and D. Forrest, "Transcriptional regulation of photoreceptor development and homeostasis in the mammalian retina," *Nature Reviews Neuroscience*, vol. 11, no. 8, pp. 563–576, 2010.
- [9] T. J. Cherry, J. M. Trimarchi, M. B. Stadler, and C. L. Cepko, "Development and diversification of retinal amacrine interneurons at single cell resolution," *Proceedings of the National Academy of Sciences of the United States of America*, vol. 106, no. 23, pp. 9495–9500, 2009.
- [10] E. M. Morrow, C. M. A. Chen, and C. L. Cepko, "Temporal order of bipolar cell genesis in the neural retina," *Neural Development*, vol. 3, no. 1, p. 2, 2008.
- [11] J. A. Brzezinski, L. Prasov, and T. Glaser, "Math5 defines the ganglion cell competence state in a subpopulation of retinal progenitor cells exiting the cell cycle," *Developmental Biology*, vol. 365, no. 2, pp. 395–413, 2012.
- [12] B. P. Hafler, N. Surzenko, K. T. Beier, C. Punzo, J. M. Trimarchi, J. H. Kong, and C. L. Cepko, "Transcription factor Olig2 defines subpopulations of retinal progenitor cells biased toward specific cell fates," *Proceedings of the National Academy of Sciences of the United States of America*, vol. 109, no. 20, pp. 7882–7887, 2012.
- [13] S. Blackshaw, S. Harpavat, J. Trimarchi, L. Cai, H. Huang, W. P. Kuo, G. Weber, K. Lee, R. E. Fraioli, S.-H. Cho, R. Yung, E. Asch, L. Ohno-Machado, W. H. Wong, and C. L. Cepko, "Genomic Analysis of Mouse Retinal Development," *PLoS Biology*, vol. 2, no. 9, p. e247, 2004.

- [14] C. Dupont, D. R. Armant, and C. A. Brenner, “Epigenetics: Definition, mechanisms and clinical perspective,” *Seminars in Reproductive Medicine*, vol. 27, no. 5, pp. 351–357, 2009.
- [15] T. Suganuma and J. L. Workman, “Signals and Combinatorial Functions of Histone Modifications,” *Annual Review of Biochemistry*, vol. 80, pp. 473–499, 2011.
- [16] R. Straussman, D. Nejman, D. Roberts, I. Steinfeld, B. Blum, N. Benvenisty, I. Simon, Z. Yakhini, and H. Cedar, “Developmental programming of CpG island methylation profiles in the human genome,” *Nature Structural and Molecular Biology*, vol. 16, no. 5, pp. 564–571, 2009.
- [17] M. Esteller, “Cancer epigenomics: DNA methylomes and histone-modification maps,” *Nature Reviews Genetics*, vol. 8, no. 4 pp. 286–298, 2007.
- [18] M. Esteller, “Epigenetic gene silencing in cancer: The DNA hypermethylome,” *Human Molecular Genetics*, vol. 16, no. R1, pp. R50–R59, 2007.
- [19] R. K. Tittle, R. Sze, A. Ng, R. J. Nuckels, M. E. Swartz, R. M. Anderson, J. Bosch, D. Y. R. Stainier, J. K. Eberhart, and J. M. Gross, “Uhrf1 and Dnmt1 are required for development and maintenance of the zebrafish lens,” *Developmental Biology*, vol. 350, no. 1, pp. 50–63, 2011.
- [20] M. Bostick, K. K. Jong, P. O. Estève, A. Clark, S. Pradhan, and S. E. Jacobsen, “UHRF1 plays a role in maintaining DNA methylation in mammalian cells,” *Science*, vol. 317, no. 5845, pp. 1760–1764, 2007.
- [21] C. Bronner, G. Fuhrmann, F. L. Chédin, M. Macaluso, and S. Dhe-Paganon, “UHRF1 links the histone code and DNA methylation to ensure faithful epigenetic memory inheritance,” *Genetics and Epigenetics*, vol. 2009, no. 2, pp. 29–36, 2009.
- [22] C. M. Rivera and B. Ren, “Mapping human epigenomes,” *Cell*, vol. 155, no. 1, pp. 39–55, 2013.
- [23] D. Huertas, R. Sendra, and P. Muñoz, “Chromatin dynamics coupled to DNA repair,” *Epigenetics*, vol. 4, no. 1, pp. 31–42, 2009.
- [24] T. Kouzarides, “Chromatin Modifications and Their Function,” *Cell*, vol. 128, no. 4, pp. 693–705, 2007.
- [25] A. Jambhekar, A. Dhall, and Y. Shi, “Roles and regulation of histone methylation in animal development,” *Nature Reviews Molecular Cell Biology*, vol. 20, no. 10, pp. 625–641, 2019.
- [26] B. Li, M. Carey, and J. L. Workman, “The Role of Chromatin during Transcription,” *Cell*, vol. 128, no. 4. Cell, pp. 707–719, 2007.
- [27] R. Karlič, H. R. Chung, J. Lasserre, K. Vlahoviček, and M. Vingron, “Histone modification levels are predictive for gene expression,” *Proceedings of the National Academy of Sciences of the United States of America*, vol. 107, no. 7, pp. 2926–2931, 2010.
- [28] A. J. Ruthenburg, C. D. Allis, and J. Wysocka, “Methylation of Lysine 4 on Histone H3: Intricacy of Writing and Reading a Single Epigenetic Mark,” *Molecular Cell*, vol. 25, no. 1, pp. 15–30, 2007.

- [29] Y. B. Schwartz and V. Pirrotta, “Polycomb silencing mechanisms and the management of genomic programmes,” *Nature Reviews Genetics*, vol. 8, no. 1, pp. 9–22, 2007.
- [30] L. Simó-Riudalbas and M. Esteller, “Targeting the histone orthography of cancer: drugs for writers, erasers and readers,” *British Journal of Pharmacology*, vol. 172, no. 11, pp. 2716–2732, 2015.
- [31] C. N. Vallianatos and S. Iwase, “Disrupted intricacy of histone H3K4 methylation in neurodevelopmental disorders,” *Epigenomics*, vol. 7, no. 3, pp. 503–518, 2015.
- [32] S. K. T. Ooi, C. Qiu, E. Bernstein, K. Li, D. Jia, Z. Yang, H. Erdjument-Bromage, P. Tempst, S.-P. Lin, C. D. Allis, X. Cheng, and T. H. Bestor, “DNMT3L connects unmethylated lysine 4 of histone H3 to de novo methylation of DNA,” *Nature*, vol. 448, no. 7154, pp. 714–717, 2007.
- [33] M. Tachibana, Y. Matsumura, M. Fukuda, H. Kimura, and Y. Shinkai, “G9a/GLP complexes independently mediate H3K9 and DNA methylation to silence transcription,” *EMBO Journal*, vol. 27, no. 20, pp. 2681–2690, 2008.
- [34] J. P. Thomson, P. J. Skene, J. Selfridge, T. Clouaire, J. Guy, S. Webb, A. R. W. Kerr, A. Deaton, R. Andrews, K. D. James, D. J. Turner, R. Illingworth, and A. Bird, “CpG islands influence chromatin structure via the CpG-binding protein Cfp1,” *Nature*, vol. 464, no. 7291, pp. 1082–1086, 2010.
- [35] K. Y. Kim, Y. Tanaka, J. Su, B. Cakir, Y. Xiang, B. Patterson, J. Ding, Y. W. Jung, J. J. H. Kim, E. Hysolli, H. Lee, R. Dajani, J. J. H. Kim, M. Zhong, J. H. Lee, D. Skalnik, J. M. Lim, G. J. Sullivan, J. Wang, and I. H. Park, “Uhrf1 regulates active transcriptional marks at bivalent domains in pluripotent stem cells through Setd1a,” *Nature Communications*, vol. 9, no. 1, p. 2583, 2018.
- [36] X. Corso-Díaz, C. Jaeger, V. Chaitankar, and A. Swaroop, “Epigenetic control of gene regulation during development and disease: A view from the retina,” *Progress in Retinal and Eye Research*, vol. 65, pp. 1–27, 2018.
- [37] L. Zelinger and A. Swaroop, “RNA Biology in Retinal Development and Disease,” *Trends in Genetics*, vol. 34, no. 5, pp. 341–351, 2018.
- [38] T. Iwagawa and S. Watanabe, “Molecular mechanisms of H3K27me3 and H3K4me3 in retinal development,” *Neuroscience research*, vol. 138, pp. 43–48, 2018.
- [39] A. Iida, T. Iwagawa, Y. Baba, S. Satoh, Y. Mochizukil, H. Nakauchi, T. Furukawa, H. Koseki, A. Murakami, and S. Watanabe, “Roles of histone H3K27 trimethylase Ezh2 in retinal proliferation and differentiation,” *Developmental Neurobiology*, vol. 75, no. 9, pp. 947–960, 2015.
- [40] D. Umutoni, T. Iwagawa, Y. Baba, A. Tsuchiko, H. Honda, M. Aihara, and S. Watanabe, “H3K27me3 demethylase UTX regulates the differentiation of a subset of bipolar cells in the mouse retina,” *Genes to Cells*, vol. 25, no. 6, pp. 402–412, 2020.
- [41] E. Shen, H. Shulha, Z. Weng, and S. Akbarian, “Regulation of histone H3K4 methylation in brain development and disease,” *Philosophical Transactions of the Royal Society B: Biological Sciences*, vol. 369, no. 1652, 2014.

- [42] H. Hao, D. S. Kim, B. Klocke, K. R. Johnson, K. Cui, N. Gotoh, C. Zang, J. Gregorski, L. Gieser, W. Peng, Y. Fann, M. Seifert, K. Zhao, and A. Swaroop, "Transcriptional regulation of rod photoreceptor homeostasis revealed by in vivo NRL targetome analysis," *PLoS Genetics*, vol. 8, no. 4, 2012.
- [43] K. Ueno, T. Iwagawa, H. Kuribayashi, Y. Baba, H. Nakauchi, A. Murakami, M. Nagasaki, Y. Suzuki, and S. Watanabe, "Transition of differential histone H3 methylation in photoreceptors and other retinal cells during retinal differentiation," *Scientific Reports*, vol. 6, p. 29264, 2016.
- [44] A. Shilatifard, "The COMPASS family of histone H3K4 methylases: Mechanisms of regulation in development and disease pathogenesis," *Annual Review of Biochemistry*, vol. 81, pp. 65–95, 2012.
- [45] J. R. Davie, W. Xu, and G. P. Delcuve, "Histone H3K4 trimethylation: Dynamic interplay with pre-mRNA splicing1," *Biochemistry and Cell Biology*, vol. 94, no. 1, pp. 1–11, 2015.
- [46] Q. Qu, Y. hei Takahashi, Y. Yang, H. Hu, Y. Zhang, J. S. Brunzelle, J. F. Couture, A. Shilatifard, and G. Skiniotis, "Structure and Conformational Dynamics of a COMPASS Histone H3K4 Methyltransferase Complex," *Cell*, vol. 174, no. 5, pp. 1117-1126.e12, 2018.
- [47] N. T. Crump and T. A. Milne, "Why are so many MLL lysine methyltransferases required for normal mammalian development?," *Cellular and Molecular Life Sciences*, vol. 76, no. 15, pp. 2885–2898, 2019.
- [48] A. Kranz and K. Anastassiadis, "The role of SETD1A and SETD1B in development and disease," *Biochimica et Biophysica Acta - Gene Regulatory Mechanisms*, vol. 1863, no. 8, p. 194578, 2020.
- [49] A. S. Bledau, K. Schmidt, K. Neumann, U. Hill, G. Ciotta, A. Gupta, D. C. Torres, J. Fu, A. Kranz, A. F. Stewart, and K. Anastassiadis, "The H3K4 methyltransferase Setd1a is first required at the epiblast stage, whereas Setd1b becomes essential after gastrulation," *Development (Cambridge)*, vol. 141, no. 5, pp. 1022–1035, 2014.
- [50] M. R. Higgs, K. Sato, J. J. Reynolds, S. Begum, R. Bayley, A. Goula, A. Vernet, K. L. Paquin, D. G. Skalnik, W. Kobayashi, M. Takata, N. G. Howlett, H. Kurumizaka, H. Kimura, and G. S. Stewart, "Histone Methylation by SETD1A Protects Nascent DNA through the Nucleosome Chaperone Activity of FANCD2," *Molecular Cell*, vol. 71, no. 1, pp. 25-41.e6, 2018.
- [51] K. Tajima, S. Matsuda, T. Yae, B. J. Drapkin, R. Morris, M. Boukhali, K. Niederhoffer, V. Comaills, T. Dubash, L. Nieman, H. Guo, N. K. C. Magnus, N. Dyson, T. Shioda, W. Haas, D. A. Haber, and S. Maheswaran, "SETD1A protects from senescence through regulation of the mitotic gene expression program," *Nature Communications*, vol. 10, no. 1, pp. 1–13, 2019.
- [52] T. Hoshii, P. Cifani, Z. Feng, C. H. Huang, R. Koche, C. W. Chen, C. D. Delaney, S. W. Lowe, A. Kentsis, and S. A. Armstrong, "A Non-catalytic Function of SETD1A Regulates Cyclin K and the DNA Damage Response," *Cell*, vol. 172, no. 5, pp. 1007-1021.e17, 2018.

- [53] J. Mukai, E. Cannavò, G. W. Crabtree, Z. Sun, A. Diamantopoulou, P. Thakur, C. Y. Chang, Y. Cai, S. Lomvardas, A. Takata, B. Xu, and J. A. Gogos, “Recapitulation and Reversal of Schizophrenia-Related Phenotypes in Setd1a-Deficient Mice,” *Neuron*, vol. 104, no. 3, pp. 471–487.e12, 2019.
- [54] A. Takata, B. Xu, I. Ionita-Laza, J. L. Roos, J. A. Gogos, and M. Karayiorgou, “Loss-of-Function Variants in Schizophrenia Risk and SETD1A as a Candidate Susceptibility Gene,” *Neuron*, vol. 82, no. 4, pp. 773–780, 2014.
- [55] T. Singh, M. I. Kurki, D. Curtis, S. M. Purcell, L. Crooks, J. McRae, J. Suvisaari, H. Chheda, D. Blackwood, G. Breen, O. Pietilinen, S. S. Gerety, M. Ayub, M. Blyth, T. Cole, D. Collier, E. L. Coomber, N. Craddock, M. J. Daly, J. Danesh, J. C. Barrett, “Rare loss-of-function variants in SETD1A are associated with schizophrenia and developmental disorders,” *Nature Neuroscience*, vol. 19, no. 4, pp. 571–577, 2016.
- [56] A. Takata, B. Xu, I. Ionita-Laza, J. L. Roos, J. A. Gogos, and M. Karayiorgou, “Loss-of-Function Variants in Schizophrenia Risk and SETD1A as a Candidate Susceptibility Gene,” *Neuron*, vol. 82, no. 4, pp. 773–780, 2014.
- [57] K. Nagahama, K. Sakoori, T. Watanabe, Y. Kishi, K. Kawaji, and M. Koebis, “Article Setd1a Insufficiency in Mice Attenuates Excitatory Synaptic Function and Recapitulates Schizophrenia- Related Behavioral Abnormalities II Setd1a Insufficiency in Mice Attenuates Excitatory Synaptic Function and Recapitulates Schizophrenia-Related ,” *Cell Reports*, vol. 32, no. 11, p. 108126, 2020.
- [58] S. Satoh, K. Tang, A. Iida, M. Inoue, T. Kodama, S. Y. Tsai, M. J. Tsai, Y. Furuta, and S. Watanabe, “The spatial patterning of mouse cone opsin expression is regulated by bone morphogenetic protein signaling through downstream effector COUP-TF nuclear receptors,” *Journal of Neuroscience*, vol. 29, no. 40, pp. 12401–12411, 2009.
- [59] Y. Tabata, Y. Ouchi, H. Kamiya, T. Manabe, K. Arai, and S. Watanabe, “Specification of the Retinal Fate of Mouse Embryonic Stem Cells by Ectopic Expression of Rx/rax, a Homeobox Gene,” *Molecular and Cellular Biology*, vol. 24, no. 10, pp. 4513–4521, 2004.
- [60] A. Iida, T. Shinoe, Y. Baba, H. Mano, S. Watanabe, Y. Tabata, Y. Ouchi, H. Kamiya, T. Manabe, K. Arai, and S. Watanabe, “Dicer plays essential roles for retinal development by regulation of survival and differentiation,” *Investigative Ophthalmology and Visual Science*, vol. 52, no. 10, pp. 4513–4521, 2004.
- [61] T. Shinoe, H. Kuribayashi, H. Saya, M. Seiki, H. Aburatani, and S. Watanabe, “Identification of CD44 as a cell surface marker for Müller glia precursor cells,” *Journal of Neurochemistry*, vol. 115, no. 6, pp. 1633–1642, 2010.
- [62] R. Patro, G. Duggal, M. I. Love, R. A. Irizarry, and C. Kingsford, “Salmon provides fast and bias-aware quantification of transcript expression,” *Nature Methods*, vol. 14, no. 4, pp. 417–419, 2017.
- [63] N. L. Bray, H. Pimentel, P. Melsted, and L. Pachter, “Near-optimal probabilistic RNA-seq quantification,” *Nature Biotechnology*, vol. 34, no. 5, pp. 525–527, 2016.

- [64] D. W. Huang, B. T. Sherman, and R. A. Lempicki, "Systematic and integrative analysis of large gene lists using DAVID bioinformatics resources," *Nature Protocols*, vol. 4, no. 1, pp. 44–57, 2009.
- [65] D. W. Huang, B. T. Sherman, and R. A. Lempicki, "Bioinformatics enrichment tools: Paths toward the comprehensive functional analysis of large gene lists," *Nucleic Acids Research*, vol. 37, no. 1, pp. 1–13, 2009.
- [66] A. Iida, T. Iwagawa, H. Kuribayashi, S. Satoh, Y. Mochizuki, Y. Baba, H. Nakauchi, T. Furukawa, H. Koseki, A. Murakami, and S. Watanabe, "Histone demethylase Jmjd3 is required for the development of subsets of retinal bipolar cells," *Proceedings of the National Academy of Sciences of the United States of America*, vol. 111, no. 10, pp. 3751–3756, 2014.
- [67] I. Aldiri, B. Xu, L. Wang, X. Chen, D. Hiler, L. Griffiths, M. Valentine, A. Shirinifard, S. Thiagarajan, A. Sablauer, M. E. Barabas, J. Zhang, D. Johnson, S. Frase, X. Zhou, J. Easton, J. Zhang, E. R. Mardis, R. K. Wilson, J. R. Downing, and M. A. Dyer, "The Dynamic Epigenetic Landscape of the Retina During Development, Reprogramming, and Tumorigenesis," *Neuron*, vol. 94, no. 3, pp. 550–568.e10, 2017.
- [68] B. Langmead and S. L. Salzberg, "Fast gapped-read alignment with Bowtie 2," *Nature Methods*, vol. 9, no. 4, pp. 357–359, 2012.
- [69] H. Li, B. Handsaker, A. Wysoker, T. Fennell, J. Ruan, N. Homer, G. Marth, G. Abecasis, and R. Durbin, "The Sequence Alignment/Map format and SAMtools," *Bioinformatics*, vol. 25, no. 16, pp. 2078–2079, 2009.
- [70] H. Li, "A statistical framework for SNP calling, mutation discovery, association mapping and population genetical parameter estimation from sequencing data," *Bioinformatics*, vol. 27, no. 21, pp. 2987–2993, 2011.
- [71] Y. Zhang, T. Liu, C. A. Meyer, J. Eeckhoute, D. S. Johnson, B. E. Bernstein, C. Nussbaum, R. M. Myers, M. Brown, W. Li, and X. S. Shirley, "Model-based analysis of ChIP-Seq (MACS)," *Genome Biology*, vol. 9, no. 9, p. R137, 2008.
- [72] G. Yu, L. G. Wang, and Q. Y. He, "ChIP seeker: An R/Bioconductor package for ChIP peak annotation, comparison and visualization," *Bioinformatics*, vol. 31, no. 14, pp. 2382–2383, 2015.
- [73] S. B. Rothbart, K. Krajewski, N. Nady, W. Tempel, S. Xue, A. I. Badeaux, D. Barsyte-Lovejoy, J. Y. Martinez, M. T. Bedford, S. M. Fuchs, C. H. Arrowsmith, and B. D. Strahl, "Association of UHRF1 with methylated H3K9 directs the maintenance of DNA methylation," *Nature Structural and Molecular Biology*, vol. 19, no. 11, pp. 1155–1160, 2012.
- [74] S. B. Rothbart, B. M. Dickson, M. S. Ong, K. Krajewski, S. Houliston, D. B. Kireev, C. H. Arrowsmith, and B. D. Strahl, "Multivalent histone engagement by the linked tandem tudor and PHD domains of UHRF1 is required for the epigenetic inheritance of DNA methylation," *Genes and Development*, vol. 27, no. 11, pp. 1288–1298, 2013.

- [75] J. Y. Hahm, J. W. Park, J. Y. Kang, J. Park, C. H. Kim, J. Y. Kim, N. C. Ha, J. W. Kim, and S. B. Seo, “Acetylation of UHRF1 Regulates Hemi-methylated DNA Binding and Maintenance of Genome-wide DNA Methylation,” *Cell Reports*, vol. 32, no. 4, p. 107958, 2020.
- [76] K. J. Wahlin, R. A. Enke, J. A. Fuller, G. Kalesnykas, D. J. Zack, and S. L. Merbs, “Epigenetics and cell death: DNA hypermethylation in programmed retinal cell death,” *PLoS ONE*, vol. 8, no. 11, p. e79140, 2013.
- [77] M. Swe and K. H. Sit, “zVAD-fmk and DEVD-cho induced late mitosis arrest and apoptotic expressions,” *Apoptosis*, vol. 5, no. 1, pp. 29–36, 2000.
- [78] T. Iwagawa and S. Watanabe, “Molecular mechanisms of H3K27me3 and H3K4me3 in retinal development,” *Neuroscience Research*, vol. 138, pp. 43–48, 2019.
- [79] T. Iwagawa, H. Honda, and S. Watanabe, “Jmjd3 plays pivotal roles in the proper development of early-born retinal lineages: Amacrine, horizontal, and retinal ganglion cells,” *Investigative Ophthalmology and Visual Science*, vol. 61, no. 11, pp. 43–43, 2020.
- [80] D. Umutoni, T. Iwagawa, Y. Baba, A. Tsuchiko, H. Honda, M. Aihara, and S. Watanabe, “H3K27me3 demethylase UTX regulates the differentiation of a subset of bipolar cells in the mouse retina,” *Genes to Cells*, vol. 25, no. 6, pp. 402–412, 2020.
- [81] C. Kizilyaprak, D. Spehner, D. Devys, and P. Schultz, “In Vivo chromatin organization of mouse rod photoreceptors correlates with histone modifications,” *PLoS ONE*, vol. 5, no. 6, p. e11039, 2010.
- [82] J. H. Lee and D. G. Skalnik, “Rbm15-Mkl1 interacts with the Setd1b histone H3-Lys4 methyltransferase via a SPOC domain that is required for cytokine-independent proliferation,” *PLoS ONE*, vol. 7, no. 8, p. e42965, 2012.
- [83] R. K. Singh, R. K. Mallela, A. Hayes, N. R. Dunham, M. E. Hedden, R. A. Enke, R. N. Fariss, H. Sternberg, M. D. West, and I. O. Nasonkin, “Dnmt1, Dnmt3a and Dnmt3b cooperate in photoreceptor and outer plexiform layer development in the mammalian retina,” *Experimental Eye Research*, vol. 159, pp. 132–146, 2017.
- [84] K. D. Rhee, J. Yu, C. Y. Zhao, G. Fan, and X. J. Yang, “Dnmt1-dependent DNA methylation is essential for photoreceptor terminal differentiation and retinal neuron survival,” *Cell Death and Disease*, vol. 3, no. 11, p. e427, 2012.
- [85] G. Chen, Y. Luo, K. Warncke, Y. Sun, D. S. Yu, H. Fu, M. Behera, S. S. Ramalingam, P. W. Doetsch, D. M. Duong, M. Lammers, W. J. Curran, and X. Deng, “Acetylation regulates ribonucleotide reductase activity and cancer cell growth,” *Nature Communications*, vol. 10, no. 1, pp. 1–16, 2019.
- [86] P. F. Liu, C. F. Chen, C. W. Shu, H. M. Chang, C. H. Lee, H. H. Liou, L. P. Ger, C. L. Chen, and B. H. Kang, “UBE2C is a Potential Biomarker for Tumorigenesis and Prognosis in Tongue Squamous Cell Carcinoma,” *Diagnostics*, vol. 10, no. 9, p. 674, 2020.
- [87] K. Zhang, W. Lin, J. A. Latham, G. M. Riefler, J. M. Schumacher, C. Chan, K. Tatchell, D. H. Hawke, R. Kobayashi, and S. Y. R. Dent, “The Set1

- methyltransferase opposes Ipl1 Aurora kinase functions in chromosome segregation,” *Cell*, vol. 122, no. 5, pp. 723–734, 2005.
- [88] D. R. Lorenz, I. V. Mikheyeva, P. Johansen, L. Meyer, A. Berg, S. I. S. Grewal, and H. P. Cam, “CENP-B Cooperates with Set1 in Bidirectional Transcriptional Silencing and Genome Organization of Retrotransposons,” *Molecular and Cellular Biology*, vol. 32, no. 20, pp. 4215–4225, 2012.
 - [89] M. Hödl and K. Basler, “Transcription in the absence of histone H3.2 and H3K4 methylation,” *Current Biology*, vol. 22, no. 23, pp. 2253–2257, 2012.
 - [90] T. Clouaire, S. Webb, P. Skene, R. Illingworth, A. Kerr, R. Andrews, J. H. Lee, D. Skalnik, and A. Bird, “Cfp1 integrates both CpG content and gene activity for accurate H3K4me3 deposition in embryonic stem cells,” *Genes and Development*, vol. 26, no. 15, pp. 1714–1728, 2012.
 - [91] K. Arndt, A. Kranz, J. Fohgrub, A. Jolly, A. S. Bledau, M. Di Virgilio, M. Lesche, A. Dahl, T. Höfer, A. F. Stewart, and C. Waskow, “SETD1A protects HSCs from activation-induced functional decline in vivo,” *Blood*, vol. 131, no. 12, pp. 1311–1324, 2018.

Acknowledgements

Firstly, I would like to express my utmost appreciation to my supervisor – Professor Sumiko Watanabe for offering me an opportunity to undertake this PhD study and providing generous supports. Without her complete trust and continuous encouragement, I would not be able to commence this PhD program, let alone having such great scientific experience. Always and forever, I will remember Sumiko sensei and our laboratory.

Secondly, I am sincerely grateful to my advisor – Dr. Toshiro Iwagawa for his perfect scientific knowledge teaching, effective guidance, and invaluable inspiration throughout the whole process, all of which are essential for the completion of this thesis and my PhD program.

Thirdly, I would like to thank Professor Yutaka Suzuki and Dr. Masaya Fukushima for their contribution to this thesis, and all the other lovely lab members for their always generous help.

I would also like to acknowledge my country China and the China Scholarship Council (CSC) for providing sufficient scholarship that supports my living here in Japan.

Last but by no means least, my heartfelt thanks go to my parents – Deng yuanwen and Luo lin – for their deep love and wholehearted support, which inspired me to pursue my ideal, and to be a better person.